DEVELOPMENT OF CO_2 INHALING BIO-HEALABLE CONCRETE WITH ENHANCED IMMUNITY TO CORROSION

Final Year Project UG 2015

By

Ibrahim Sarwar

Hamza Miraj

Wajeeh Ud Din Ahmed

Hassan Ali Subhani

Supervisor

Asst. Prof. Dr. Rao Arsalan Khushnood

NUST Institute of Civil Engineering

School of Civil and Environmental Engineering

National University of Sciences and Technology, Islamabad

Pakistan

2019

Development of CO_2 Inhaling Bio-Healable Concrete with Enhanced Immunity to Corrosion

Final Year Project UG 2015

By

Ibrahim Sarwar	00000 127739
Hamza Miraj	00000 120007
Wajeeh Ud Din Ahmed	00000 122327
Hassan Ali Subhani	00000 131954

NUST Institute of Civil Engineering

School of Civil and Environmental Engineering

National University of Sciences and Technology, Islamabad

Pakistan

2019

This is to certify that the

Final Year Project Titled

"Development of CO_2 Inhaling Bio-Healable Concrete with Enhanced Immunity to Corrosion"

Submitted By

Ibrahim Sarwar	00000 127739
Hamza Miraj	00000 120007
Wajeeh Ud Din Ahmed	00000 122327
Hassan Ali Subhani	00000 131954

has been accepted towards the requirements

for the undergraduate degree

in

CIVIL ENGINEERING

_____

Dr. Rao Arsalan Khushnood
Head of Structural Engineering Department
NUST Institute of Civil Engineering
School of Civil and Environmental Engineering
National University of Sciences and Technology, Islamabad

ACKNOWLEDGEMENTS

In the name of Allah, the most Beneficent, the most Merciful as well as peace and blessings upon Prophet Muhammad, His servant and final messenger.

We are first and foremost, extremely grateful to Allah Almighty for enabling us to complete our research project and without Whose willingness we could not have imagined to accomplish such an enormous task.

The efforts and sacrifices that our parents and teachers have made over the course of our lives to reach where we stand today are highly acknowledged. Special mention of our siblings who were a source of constant motivation and stood by our sides during tough times.

We respect and appreciate the efforts put up by our supervisor Dr. Rao Arsalan Khushnood, Head of Structural Engineering Department. His valuable advice and research commitments were a source of motivation for us. Throughout the research project his constant support and taking time out of his busy schedule for mentorship kept us proceeding forward. Moreover, his professional grooming of the group in thesis writing and presentation is valuable and something that will help us in our practical life.

We would express our gratitude towards Dr. Shahid, HoD Materials Engineering, SCME, NUST for allowing us to carry out the corrosion tests as well as Dr. Zeeshan Ali Khan, IESE, NUST providing expertise in development of climate control chamber and permitting us to use the pyrolysis setup. We are thankful to the lab staff of mentioned departments for their assistance in performing the lab tests.

We are extremely grateful to Ms. Nafeesa Shaheen, PG student at NICE, for providing us bacterial culture as well as guiding us throughout the research and practical phase of the project. We value the assistance provided by the entire staff (Mr Riasat, Faheem, Abdullah and Ismail) of Structures Lab, NICE and Mr. Ahmed of Geotech Lab. Special thanks to Lab Engr. Mati Ullah Shah and Atif Mehmood in coordinating for our testing.

Finally, we would extend our appreciation towards our friends and colleagues who kept encouraging us and provided necessary assistance in completion of this research project.

Dedication

To

Our Advisor Dr. Rao Arsalan Khushnood

& Our Families

ABSTRACT

Urbanization trend in Pakistan over the decades has increased abruptly which calls for increased construction to meet the demands of ever-growing population. Construction sector is one of the major contributors of CO_2 emissions that has led to world facing global warming issues. Since concrete is a popular construction material primarily because of its strength, it has the tendency to develop micro structural cracks that gradually deteriorates its properties owing to embedded reinforcement exposed to chloride ions that leads to corrosion. Self-healing is potential remedy to this problem. Various researches have been conducted to investigate self-healing and bio-influenced self-healing has been concluded to be the best approach in terms of crack healing and strength recovery. Bio-influenced self-healing can be achieved by immobilizing bacteria in nano/micro fillers such as carbonized char, but most of these fillers are incompatible with alkaline concrete environment rendering the effectiveness of long-term healing. In this research study, nano/micro carbonized char was used to examine healing activity at various ages, investigate the corrosion potential and quantifying CO_2 sequestration ability of self-healing concrete. Scanning Electron Microscopy (SEM), X-ray Diffraction (XRD), Thermogravimetric Analysis (TGA) and Optical Microscopy were conducted to verify self-healing. Corrosion was examined through Tafel Polarization, Weight Loss Measurement, Sorptivity test and Non-Steady State Chloride Ion Migration Coefficient Experiment. CO_2 sequestration ability was quantified by developing a climate monitoring chamber. Experimental results reveal that carbonized char is an effective carrier to immobilize bacteria with maximum healing reported to be 4 mm having a strength recovery of 96.3%. corrosion reduction potential was found to be 82% and CO_2 sequestration ability of self-healing concrete was 3 times compared with a normal concrete.

TABLE OF CONTENTS

LIST OF FIGURES

LIST OF TABLES

LIST OF ACRONYMS

ASTM	American Society of Testing and Materials
CWMA	Crack Width Measurement Analysis
CWT	Carbonized Waste Char
EDS	Energy Dispersive Spectroscopy
fc’	Compressive Strength
GNP	Graphite Nano Particles
LWA	Light Weight Aggregates
OM	Optical Microscopy
SEM	Scanning Electron Microscopy
SRI	Strength Recovery Index
TGA	Thermogravimetric Analysis
UPV	Ultrasonic Pulse Velocity
UTM	Universal Testing Machine
XRD	X-Ray Diffraction

CHAPTER 1

INTRODUCTION

1.1 General

Concrete being a composite material has been widely utilized in construction sector due to its plasticity, hydraulicity, strength and toughness properties. However, production of concrete results in huge quantum of CO_2 emitted which is main source of global warming. Moreover, since it is predominantly brittle in nature and bears low tensile strength, it is susceptible to progression of cracks which causes ingression of aggressive agents that are detrimental to the durability of concrete. It is estimated that the damage due to corrosion of concrete in the US is $276 billion with an annual repair cost to be $18-21 billion. In addition to that the structure also requires periodic maintenance that accounts for a significant cost. Therefore, it is essential to arrest the crack proposition to prolong the structural life of the building thus reducing the subsequent maintenance cost.

1.2 Self-Healing and Corrosion

Self-healing is an autonomous repair crack repairing technique which is not only eco-friendly but also natural driven. In bacterial inspired self-healing, once the crack is propagated the moisture seeps into the concrete where bacterial spores, though dormant but viable, become active through metabolism. Bacteria standalone cannot survive in concrete due to mechanical pressures and harsh alkaline environment; it needs an immobilizer consisting of nano/micro particles. Later, cracks are filled through microbial calcite precipitation, reducing further ingression of water and chloride ions. Since the permeability is reduced, it will preserve the embedded reinforcement, increasing the structural life of the building.

1.3 Environmental Impact

Construction sector accounts major contribution towards carbon footprint with production and logistics of cement being the main factor. Bacterial inspired self-healing concrete utilizes carbon dioxide from atmosphere to precipitate calcite and in addition to that the carbonized nano/micro char also has the ability to adsorb CO_2.

1.4 Problem Statement

In the past, numerous studies have been conducted to develop bio-based autonomous self-healing concrete in which different immobilizers were examined and their efficiencies compared with each other, as carrier media increases the viability of bacterial spores over time. Mostly, commercial products such as iron

oxide, bentonite, graphite etc. have been utilized that are expensive and pose some threats to concrete such as corrosion. A novel multi-functional immobilizer, readily available in nature and is waste product of some industry for which disposal still remains a challenge, is yet to be synthesized.

The effectiveness of immobilizer depends on its concentration which requires to be investigated to achieve optimum healing activity. In addition, past researches have been restricted to filling nano/micro level cracks that results in densification of concrete matrix. Effectiveness of bio-inspired self-healing in macro level (> 7mm) cracks are yet to be studied in detail.

Self-healing action involves filling of nano/micro cracks decreasing the permeability of concrete hence aggressive ions penetration into concrete matrix is restricted therefore preserving the embedded reinforcement against corrosion. As yet, no study has yet been conducted to relate the response of self-healable concrete against corrosion.

CO_2 is consumed by bacteria to precipitate calcite during its metabolic activity that essentially fills the cracks. But till date, no effort has been made to quantify the CO_2 sequestration ability of bio-influenced self-healing concrete.

1.5 Objectives

1. To investigate novel immobilizer in the form of carbonized nano/micro particles synthesized by pyrolysis of rubber tires
2. To reduce carbon footprint in order to promote sustainability
3. Enhance the immunity of reinforced concrete against corrosion with bio-based species
4. Investigate performance of bio-emulsion against conventional crack filling technique in dead concrete
5. To investigate the optimum char content for better healing efficiency, anti-corrosion

1.6 Thesis structure

Followed by introduction, a detailed literature review has been provided in chapter 2 pertaining to self-healing and corrosion within the concrete.

Chapter 3 explains the material characterization utilized in the project and in-depth experimental methodology adopted for this research study comprising of casting regime and test numbers.

The results of tests and their critical explanations have been presented in chapter 4 for self -healing, corrosion and CO_2 sequestration ability.

Chapter 5 discusses the field trial designed to investigate the performance of bio-emulsion in dead concrete along with its cost benefit analysis.

The conclusions drawn from this research work and recommendations for future study are summarized in chapter 6 of this thesis.

CHAPTER 2

LITERATURE REVIEW

2.1 SELF-HEALING

2.1.1 Characteristics of Self-Healing Behaviour

Self-healing concrete is manufactured from composite materials that have the capability to assist damaged material in their strength recovery, but the extent of damage directly affects the strength loss (Ghosh, 2005) hence affecting the recovered strength over the course of a structures service life. Since the damage detectability is difficult to predict and structures are vulnerable to sudden failure, self-healing phenomenon is particularly useful in composite material based concrete matrix (Van der Zwaag, 2010).

2.1.2 Classification Based on Self-Healing Behaviour

Based on mechanism involved to repair cracks, self-healing can be classified as either autonomous or non-autonomous (Hager, 2010). Former utilizes external stimuli heat or light for healing action to take place while in latter, damage induced triggers the crack repairing mechanism (Hager, 2010). Another form of self-healing can be intrinsic or extrinsic mode. Extrinsic self-healing involves addition of external agents such as capsules within the cementitious matrix and eruption of these capsules' releases material responsible for crack filling (Van der Zwaag, 2010).

2.1.3 Non-biological Techniques of Self-Healing

Microencapsulation techniques were adopted in the past researches (Tittelboom, 2011) (Yang, 2007) which essentially involved the release of healing material when the microcapsules busted as result of either change in pH or moisture. Healing agents like epoxy resins (Nishiwaki, 2006), alkali -silica solutions (Mihashi, 2000) were incorporated with cementitious matrix but neither material showed significant strength recovery compared with manual healing mechanisms nor drastically improve the mechanical properties because of permanent voids left at activity site (Tittelboom, 2011).

2.1.4 Bio-Influenced Self-Healing

Bio-influenced self-healing process requires deposition of calcite to fill the micro-structural cracks over period of time and researches have been conducted to

analyze the performance evaluation of calcite in enhancement of properties of cementitious matrix (Ramachandran, 2001) (Jonkers, 2007) (Khaliq, 2016).

2.1.5 Biological Process of Microbial Induced Calcite Precipitation

Calcite precipitation potential of bacterial spores is influenced by numerous factors such as surrounding pH, temperature and available nutrients. But the governing factors are 1. Calcium concentration 2. Concentration of dissolved inorganic carbon 3. pH 4. Availability of nucleation sites (Hammes & Verstraete, 2002). The bacteria decompose urea into ammonium and carbonate ions with the help of urease enzyme. The chemical reaction is as follows; (Ng et al, 2012)

$$(NH_2)^{+2} + 2H_2O \rightarrow 2NH^{+4} + {CO_3}^{-2}$$

$$Ca^{+2} + {CO_3}^{-2} \rightarrow CaCO_3$$

The release of ammonium ions via hydrolysis of urea makes surrounding environment more alkaline as result alkaline sensitive bacteria instigate the precipitation of calcite.

Figure 1 shows the schematics of self-healing process of microbial induced self-healing (Hager, 2010)

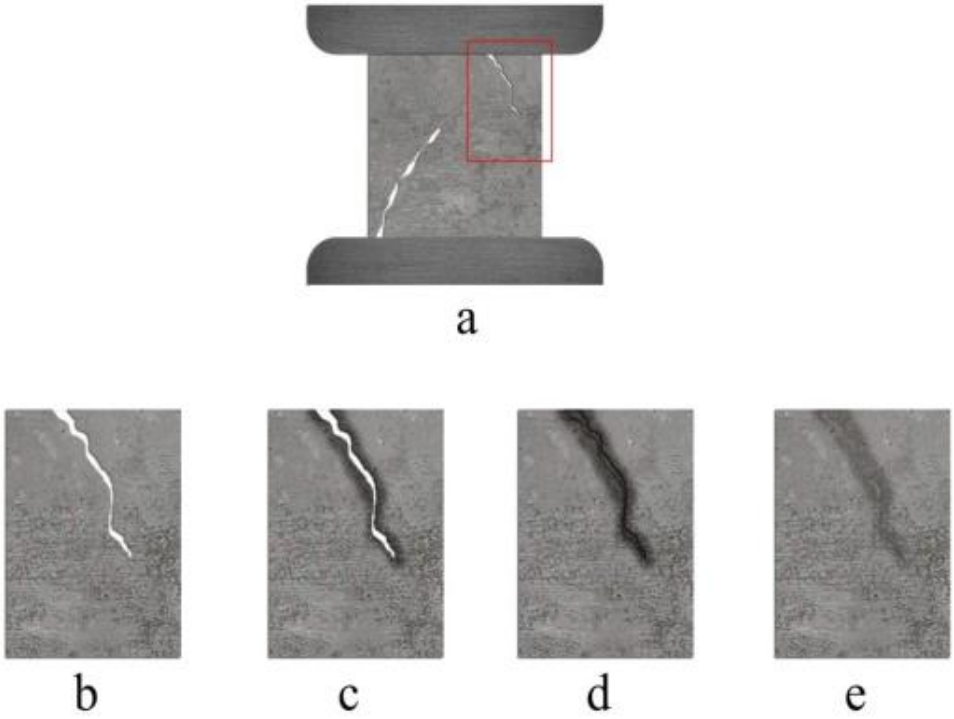

Figure 1: Stages of Crack Healing in concrete

1. Crack is formed under a mechanical load as shown in figure 1.1a
2. Figure 1.1c reflects the general principle, a mobile phase is generated that is triggered by external stimuli which in this case is damage induction.
3. Later, as seen in the figure 1.1d, mass transport takes place at damaged site adhering with crack planes by physical interaction or chemical bonds.
4. Once healing is completed, previously generated mobile phase is attained, with fully restored mechanical properties as shown in figure 1.1e

2.1.6 Influence of Type of Microorganisms

Urease positive bacteria act as catalyst in the urea hydrolysis providing an appropriate pathway for production of carbonate ions as it has the ability to alkalinize the surrounding environment (Bhasker, 2016). Researchers have utilized various species of bacteria to investigate self-healing like *Sporosarcina pasteurii* (Bang et al., 2001), (Ramakrishnan, 2005), *Bacillus sphaericus* (Ramachandran), (De Muynck et al., 2008), (Wang et al., 2011) and *Bacillus subtilis* (Khaliq, 2016) as the most commonly used bacteria in cementitious materials and concrete while *Bacillus psuedofirmus*, *Bacillus cohnii* (Jonkers and Erik Schlangen, 2014) (Jonkers, 2010) and *Bacillus alkalinitrilicus* (Wiktor and Jonkers, 2014) have also been tested to a certain level. The primary factor responsible in the selection of bacterial specie is the pH, as fresh concrete has a pH of 11-13, Bacillus subtilis has the ability to survive hostile pH conditions. In addition, these species typically form spores, which resist high mechanical and chemical induced stresses (Sagripanti and Bonifacino 1996). Moreover, they produce spores that remain dormant up to 200 years (Schlegel 1993, Jonkers 2007). Hence, the most promising bacterial spores appear to be alkaliphilic spore forming bacteria of genus bacillus (Jonkers,2010).

2.1.7 Bacterial Concentration

Not only does the bacterial type but bacterial concentration also affects the performance of microbial induced self-healing. *E.coli* with 10^5 cells/ml regarded as an ideal concentration to enhance mechanical properties by Ghosh (2007). Ramachandran (2005) has suggested 7.3×10^3 cells/ml for *Bacillus pasteurii* and 6×10^8 cells/ml for *Bacillus psuedofirmus*. For both effective self healing and enhancement of mechanical properties Nugroho(2015) has suggested 10^5 and 10^6 cells/ml as ideal bacterial concentration for bacterial specie Bacillus Subtilis.

2.1.8 Carrier Materials

Bacteria needs an immobilizer to increase its dormant period as well as to increase its healing efficiency. Poly urethane and silica gel have been widely utilized as vehicle for immobilization of enzyme (Wang, 2011). Jonkers (2010) used clay pellets as a carrier for bacteria. Wang (2012) utilized diatomaceous earth as effective carrier for aerobic and anaerobic bacteria in high pH concrete environment (Wang, 2012).

2.1.9 Influence of Nutrients

To precipitate calcite bacterial spores needs an organic precursor for which calcium lactate is considered a suitable choice (Khaliq, 2016), as it starts to dissolve during the mixing process and does not affect the setting time of concrete (Jonkers, 2010).

2.1.10 Improvements in Characteristics

Bacillus Subtilis increased the compressive strength when incorporated with LWA and GNP (Khaliq, 2016). Jonkers (2007) utilized Bacillus psuedofirmus and Bacillus cohnii for microbial induced self-healing and reported a 10% increase in compressive strength. A 17% increase in compressive strength was observed using bacterial specie sporosarcina pasteurii mortar cubes (Achal, 2009).

Sierra Beltran's (2014) evaluation of flexural strength of bio based ECC material concluded a slightly better recovery of flexural strength and deflection capacity of bio-based samples against control samples.

Achal (2011) reported significant reduction in water permeability in cement mortar cubes bearing sporosarcina pasteurii. The reason quoted by Bhasker (2016) was the denser interfacial zone formed between the aggregate and concrete mix via calcite precipitation.

2.2 CORROSION

2.2.1 Introduction

Corrosion in reinforcement is an electrochemical process whereby Fe is removed from the reinforcement and dissolves in surrounding water present in the pores of concrete, resulting in the formation of ferrous ions (Fe^{+}). These ferrous ions then combine chemically with hydroxyl ion (OH^{-}) and dissolved oxygen (O_2) to form varieties of rust that allows volume of steel to expand by six times (Mansfeld, 1981) generating stresses that initiate cracks resulting in spalling of concrete cover hence reducing the service life of the structure.

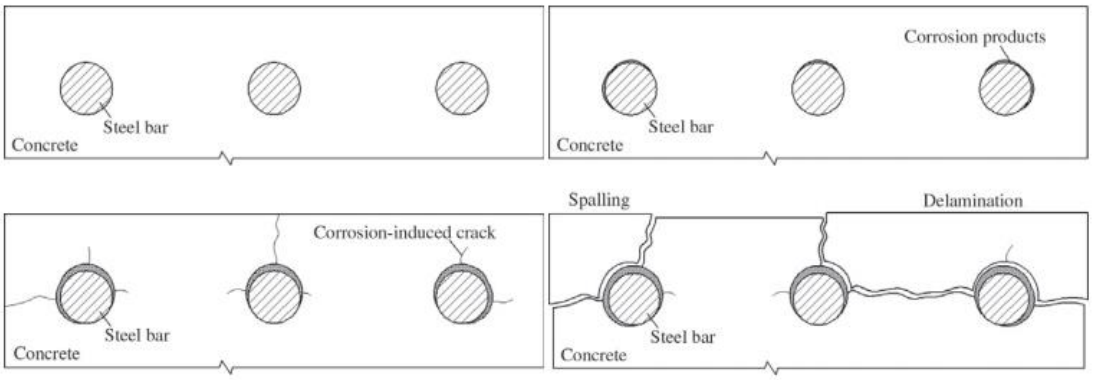

Figure 2: Stages in corrosion induced damage (a) Passive rebar. (b) Corrosion initiation and growth. (c) Further corrosion and crack propagation. (d) Spalling/delamination.

2.2.2 Corrosion Process

Process of corrosion as illustrated in the figure 3 triggers with the establishment of nucleation sites on steel bar. At anode, oxidation of Fe takes place as per the following equation

$$Fe \rightarrow Fe^{+2} + 2e^{-}$$

Electrons generated travel through the steel to cathode where reduction takes place according to the below equation

$$2e^{-} + 2H_2O + 0.5O_2 \rightarrow 2OH^{-}$$

Oxygen and moisture utilized in the above equation comes from the permeability of concrete cover and serves as an electrolyte. The formation of rust according to Broomfield (1997) occurs through the following stages

$$Fe + OH^{-} \rightarrow Fe(OH)_2 \quad Ferrous\ hydroxide$$

$$4Fe(OH)_2 + O_2 + 2H_2O \rightarrow 4Fe(OH)_3 \quad Ferric\ hydroxide$$

$$Fe(OH)_3 \rightarrow Fe_2O_3.H_2O + H_2O \quad Hydrated\ ferric\ oxide\ (rust)$$

Rust being brittle is reddish brown in colour and its stains can be visible on cracked concrete as well.

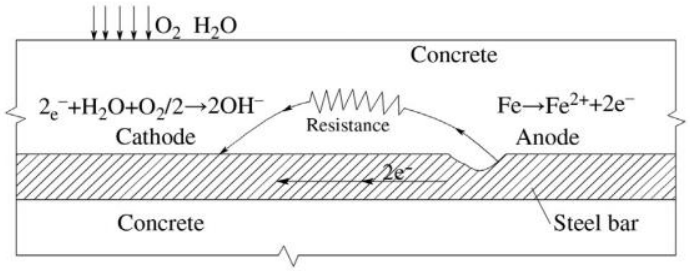

Figure 3: Schematics of corrosion process

2.2.3 Corrosion Rate

An important governing factor regarding corrosion rate is the availability of dissolved oxygen around the cathodic site (Bentur A, 1997). If the supply of dissolved oxygen is not continuous it inhibits the corrosion reaction and for this reason concrete cover is provided for reinforcement as reduces the seepage of dissolved oxygen to prevent corrosion. In such case the rate of corrosion becomes "diffusion controlled" which accounts for decrease in potential between anode and cathode, a process called polarization.

Another significant factor that determines the rate of corrosion is restriction of ionic current passing through the pores of concrete. Slower the flow rate of charge carrying ionic species; lower would be the rate of corrosion reactions and this can be attained by higher electrical resistance of concrete surrounding the rebar. Lastly, a process termed passivation restricts the rate of corrosion. In dense concrete this phenomenon does not occur due to high alkalinity (pH 13) but when the concrete is exposed to pH 11.5 (depicted in the figure below) and above in presence of dissolved oxygen, the rebar reacts with it to form metal oxides/ hydroxides which are thin, dense and impenetrable. This film prevents anodic reaction renders the rate of

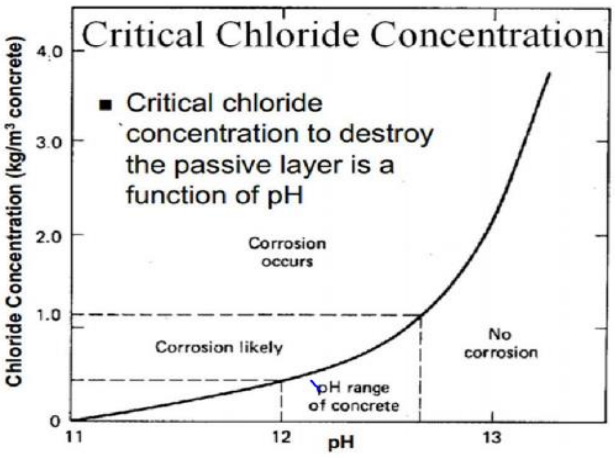

Figure 4: Relationship between Cl^- concentration and pH;
Source: Steel corrosion in concrete by Bentur et al

corrosion so slow that in some cases steel can be believed to be non-corroding. However, the breakdown of this passive layer can take place due to ingression of chloride ions or carbonation. It is worthy to mention that chloride and carbonate ions diffuse into concrete without significantly damaging it unlike sulphate ion that deteriorate concrete without harming steel.

The service life of reinforced concrete structures can be divided into two stages, the initiation stage and the propagation stage illustrated through the graph in the figure below. In the first stage reinforcement is passive but de-passivation due to chloride attack and carbonation results in corrosion. Adequate concrete cover and reduced penetration rate of above-mentioned aggressive agents prolongs the initiation stage. The second stage begins after de-passivation and end after limit state is attained whereby, the cracking of steel or spalling of concrete occurs.

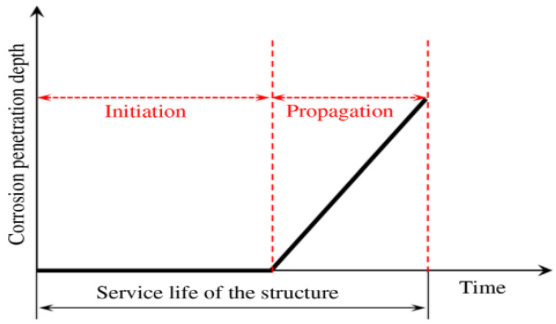

Figure 5: Relationship between Corrosion penetration depth and service life of structure

2.2.4 Carbonation-Induced Corrosion

Carbonation within the concrete causes neutralization of its alkalinity that disturbs the stable passive layer protecting the reinforcement. Carbonation starts near the surface of concrete and slowly propagates towards the inner zones reaching near-neutral pH levels through the following equations

$$CO_2 + H_2O \rightarrow H_2CO_3$$

$$Ca(OH)_2 + H_2CO_3 \rightarrow CaCO_3 + 2H_2O$$

2.2.5 Chloride-Induced Corrosion

The role of chloride attack on de-passivation is different from carbonation that primarily deals with neutralization of pH. When the chloride ions reach a minimum threshold on the surface of rebar, they start to act as a catalyst. Similar to other catalysts, chloride ions themselves are not consumed instead they accelerate the whole process via following equation

$$Fe^{+2} + 2Cl^{-} + 4H_2O \rightarrow FeCl_2.4H_2O$$

$$FeCl_2.4H_2O \rightarrow Fe(OH)_2 + 2Cl^{-} + 2H^{+} + 2H_2O$$

The reservoir of hydroxyl ions surrounding the rebar is enough to protect the passive film and a lower concentration of chloride ions would not de-passivate it. However, at a certain high concentration, the chloride ions can destroy the passive film causing pitting corrosion as illustrated in the figure.

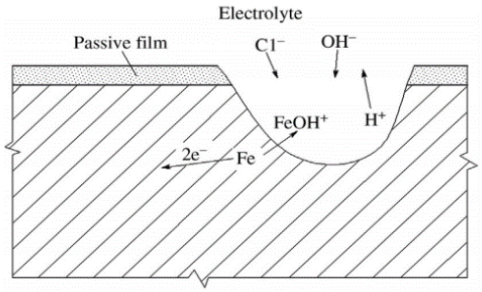

Figure 6: Chloride induced corrosion process

CHAPTER 3

MATERIAL AND EXPERIMENTAL METHODOLOGY

3.1 MATERIALS

Materials used in manufacturing of CO_2 inhaling bio healable concrete as well as their characterization are mentioned in the upcoming section followed by a detailed experimental methodology.

3.1.1 Carbonized Nano/Micro Bio-char

3.1.1.1 carbonization of waste tires

Powdered waste tire was procured from Shamsabad, Rawalpindi which was later sieved through #200 sieve set. Later carbonization was performed through pyrolysis, which involves endothermic decomposition of material at elevated temperatures that results in permanent change in physical and chemical structure of the said material. The products of pyrolysis are solid char, liquid oil and flammable gases (which can be further pre-treated).

The pyrolysis was performed in cylindrical fixed bed reactor manufactured from stainless steel. First the reactor assembly was purged with N_2, in order to remove oxygen. The raw feedstock (crushed tires) was fed into the reactor that was heated via thermocouple at 450 °C for 30 minutes using PID temperature controller with stage fixed at 20 °C per minute. As per Ahmed. Zeeshan (2018) heating above 500 °C results in more proportions of gaseous products than char and oil. The reactor was sealed in two layers (mica and ceramic wool) to provide insulation to the reactor.

Pyrolysis of scrap tires yielded 46.3% char, 23.9% oil and 29.8% gases.

3.1.1.2 milling of carbonized waste tires

Planetary Ball Milling technique was adopted that involves mechanical means to reduce particles into nano size. Stainless balls of dia 2 mm, 5 mm and 10 mm were utilized together in a stainless steel can. The ratio of feed to stainless steel balls was kept 1:20 and the machine was operated 400 ppm with char being retrieved after every 30 min.

Later laser granulometry was performed on the obtained samples to obtain the optimum milling period for CWT. Examinations reveal that for 3

Figure 7: Raw pyrolyzed WT
$D_{50} = 1.27\ mm$

hours of milling the specimen size kept on reducing after which the specimens again increased in the size.

Figure 8: Ball milled pyrolyzed WT
$D_{50} = 4.51\ \mu m$

Afterwards scanning electron microscopy (SEM), as shown in the figure below, was conducted to work out average particle size. SEM result shows char particles have irregular shape with rough edges bearing rough texture.

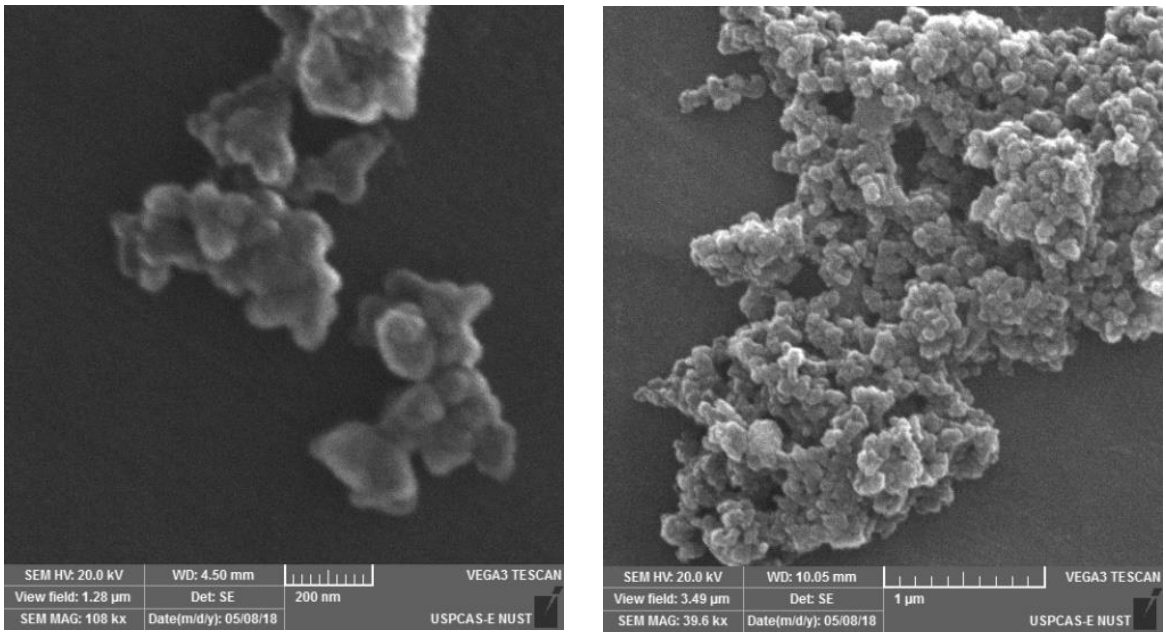

Figure 9: SEM of CWT (a) at 200 nm (b) 1 µm resolution

Energy dispersive spectroscopy (EDS) was performed for elemental characterization of carbonized waste tires shown in the figure and result summarized in the table below indicating the presence of 96.44% carbon within the CWT char.

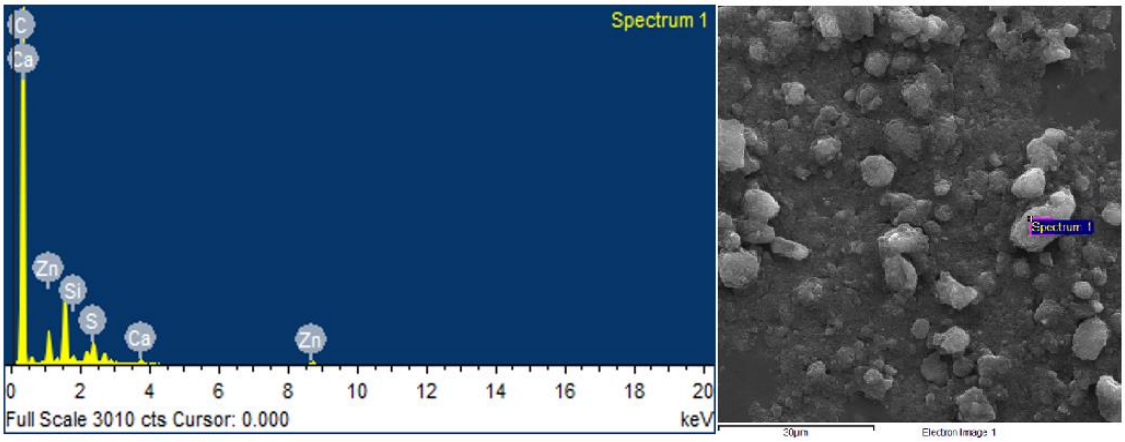

Figure 10: EDS of CWT

Table 12: Elemental composition of CWT

Element	C	Si	S	Ca	Zn
Weight %	96.44	0.32	1.21	0.28	1.75

3.1.2 Bacteria

Bacteria utilized in the research study was bacillus subtilis which is a rod shaped, gram-positive bacterium found commonly in soil. It has the ability to resist extreme pH and temperature yet forming protective endospores.

Bacillus subtilis used has American type culture collection (ATCC) number 11774 and is manufactured under ISO 9001:2008 certification. Nutrient broth used for bacteria consisted of lab-lemco powder 1.0 g/l, yeast extracts 2.0 g/l, peptone 6 g/l and sodium chloride 5.0 g/l. pH 7±0.2 All cultures were incubated aerobically at 37°C for 24 h with shaking at 250 rpm. The pure culture was maintained in liquid, on nutrient agar plate, and cryopreserved in 80% glycerol at -80°C.

The growth of bacterial spores was done in ASAB microbiology lab, where a fixed concentration of bacteria to be added was attained. For verification, a reference blank solution was prepared and absorbance of bacteria was noted through spectrophotometer. A selected wavelength of 600 nm was applied on a 0.5 ml blank

solution and after the machine had detected the blank solution it was replaced with 0.5 ml bacterial solution with again same wavelength applied over it. Ramachandran equation $Y = 8.59 \times 10^7 \times X^{1.3627}$ where "Y" is concentration of bacterial solution in cells/ml and "X" is optical density (OD) obtained from spectrophotometer. The bacterial concentration in our case was selected to be 3.3×10^7 cells/ml for casting of concrete.

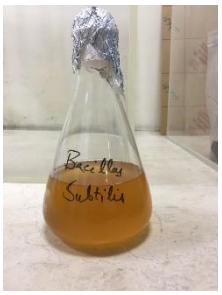

Figure 11: Prepared solution of bacillus subtilis

3.1.2.1 optical microscopy

Since CWT would act as an adhering surface for bacterial specie its interaction with it was studied using optical microscopy. The following image shows the result of compatibility test from which it can be inferred that CWT does not kill bacteria whereas, cellulose kills bacteria as evident from dark well formed around it.

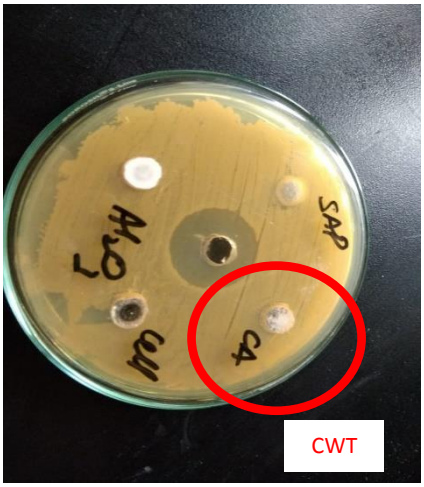

Figure 11: Result of bio-compatibility test

3.1.3 Calcium Lactate

Calcium lactate act as a food for bacteria in the precipitation of $CaCO_3$ and has been widely used in self-healing studies as reported in literature (Jonker, 2010) due to its ability to dissolve readily during mixing phase of casting. Calcium Lactate

Pentahydrate was of DAEJUNG (CAS # 5743-47-5, CAT # 2513-4405) with its

Linear Formula	*C6H10CaO6 · 5H2O; Ca (CH3CHOHCOO)2 · 5H2O*
Molecular Weight	308.3
Assay	98%
Melting Point	240 °C

properties summarized in the table below

Table 2: Properties of calcium lactate

3.1.4 Cement

Bestway grade 53 cement, preserved in a sealed container from moisture, was used in our research study. The table below lists the properties of cement.

Table 3: Properties of cement

Median Size (D50) (µm)	9.50
Final Setting (min)	135.0
Specific Gravity	3.14
Initial Setting (min)	35

3.1.5 Sand

Lawrencepur sand was used in our research bearing a fineness modulus of 2.55 which is well within the prescribed limits (2.2 to 3.2) of ASTM. The gradating curve shown in the figure below was obtained by performing the sieve analysis according to ASTM C33.

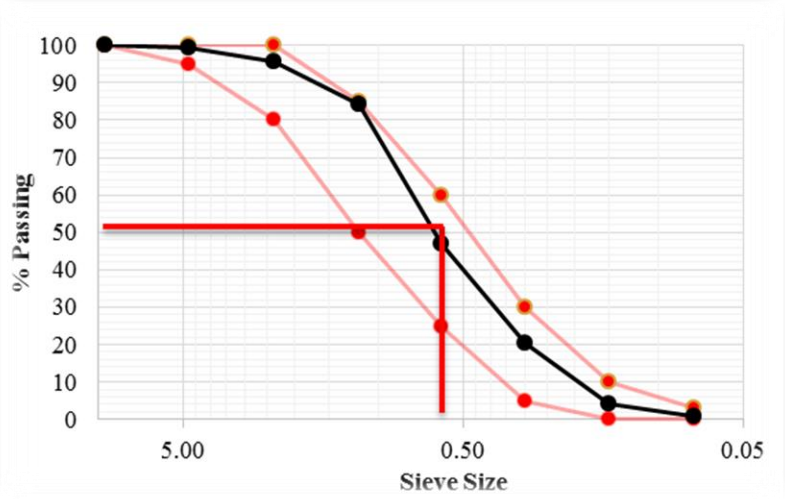

Figure 13: Particle size distribution of sand

Table 4: Properties of sand

Median Size, (D_{50}) (mm)	0.62
Fineness Modulus	2.55
Specific Gravity	2.67
Water Absorption	1.6%

3.1.6 Aggregate

The aggregate was procured from Margalla and the following table summarizes the properties of aggregate.

Table 5: Properties of aggregates

Crushing Value	22.11%
Specific Gravity	2.34
Water Absorption	0.68%

3.1.7 Steel

Karachi steel was used in our research project having following properties

Table 613: Properties of steel

Bar Size	3
Grade (ksi)	40
Yield Strength (Mpa)	351.2

3.2 EXPERIMENTAL METHODOLOGY

In order to investigate the objectives established for our research study we conducted a series of tests on 140 different concrete specimens. The table below lists the test numbers for the research work.

Table 7: Details of casting

Test	Moulds	Quantity	Formulations	Total
Bio-Healing	Cubes (4 “)	9	6	54
	Beam (4“ x4“ x 16“)	3	6	18
CO_2 Monitoring	Cubes (6”)	8	4	32
Corrosion	Cylinders (4” x 8”)	6	6	36

Before the carbonized waste tire char was added to the concrete mix it was first sonicated using sonicator for 30 min to ensure effective dispersion of char particles. The dispersion prevents the formation of agglomerates within the within the concrete samples that can affect the healing efficiency of bacteria as well as reduced compressive strength. Since the microbes were incubated at 37 °C, sonication at high temperature can greatly affect the concentration of bacteria as it can yield dead spores.

3.2.1 Mix Design

In order to formulate the mix design, literature was referred but no substantial information could be extracted. Therefore, keeping in view the properties of material and atmospheric condition e.g. humidity, temperature a mix design was devised for six different formulations as shown in the table below. Two of which are control samples, plain control sample i.e. no addition of bacteria or carbonized waste tire char and bacterial controlled sample having microbial species but no carbonized waste char. While the rest of the formulations had different proportions of carbonized waste tire char immobilized with bacteria. SIKA 520 super plasticizer was utilized to increase the workability of concrete kept 1% of the cement content. Calcium lactate 3% of cement was used in casting of concrete for bacterial and char control samples.

Table 8: Details of concrete formulations

Sample Name	Mode	Ingredients				
		Mix Design	Super Plasticizer	W/C ratio	Bacterial Concentration	Bio-Char
PCS	Plain Control	1 : 1.9 : 2.2	1%	0.4	-	-
BCS	Bacterial Control				$3.3x\ 10^7$ cells/ml	-
BIC 0.25	Bacterial Immobilized Char Control					0.25%
BIC 0.50						0.50%
BIC 0.75						0.75%
BIC 1.00						1.00%

3.2.2 Mixing Regime

Following mixing scheme, summarized in the table below, was employed for casting of concrete done using concrete mixer of NICE structures lab.

Table 9: Procedure for concrete preparation

Step 1	The materials were weighed as per the formulations
Step 2	Carbonized waste tire char was sonicated at 25 °C for 30 min prior to mixing
Step 3	Cement, sand, aggregate and calcium lactate were slow dry mixed for 45 sec
Step 4	80% water was added to the dry mix whilst mixing shaft slowly rotating for a period of 90 sec
Step 5	Remaining water mixed with bacterial solution as well as superplasticizer and sonicated carbonized waste tire char was added during the fast mixing process that lasted for 45 sec
Step 6	The concrete mix was poured into the moulds
Step 7	The moulds were placed on vibrating table for even compaction and the surface was levelled with trowel

3.2.3 Curing

After the specimens were casted, they were demolded after 24 hours and placed in the temperature-controlled curing tank at 25°C for 28 days before being ready for experimental testing. For healing tests, the specimens were cured for 3, 14 and 28 days respectively after which the specimens were pre-cracked at 85% of fc'. later they were re-cured for 28 days.

CHAPTER 4

EXPERIMENTAL TESTS AND RESULTS

4.1 SELF-HEALING ANALYSIS

4.1.1 Crack Width Measurement Analysis

CWMA is a visual technique whereby crack filling by microbial precipitation within the concrete samples is recorded using optical microscope. The samples were cured as mentioned earlier for 3, 14 and 28 days after which cracks were manually introduced using UTM at 85% of their fc'. The samples then were re-cured for 28 days after which they were inspected for their crack filling potential as summarized in the table below.

Table 10: Summary of CWMA results

SAMPLE	3D | 28D	14D | 28D	28D | 28D
PCS	No healing	No healing	No healing
BCS	Partial healing	Partial healing	Partial healing
BIC 0.25	2.2	2.5	2.8
BIC 0.50	2.4	2.6	3.1
BIC 0.75	2.7	3.1	4.0
BIC 1.00	2.6	3.3	3.6

Figure 14: OM image of PCS

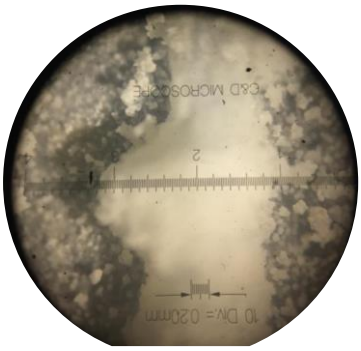

Figure 151: OM image of BCS

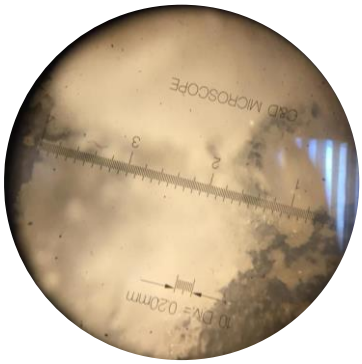

Figure 162: OM image of BCS 0.25

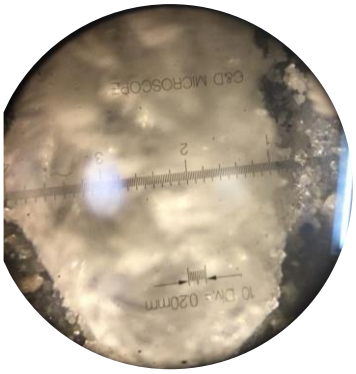

Figure 17: OM image of BCS 0.50

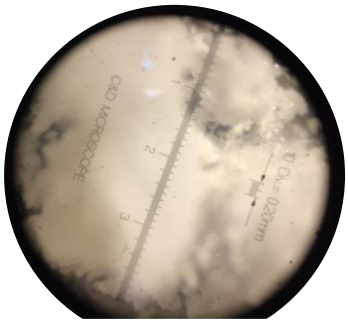

Figure 18: OM of BCS 0.75

The first and foremost deduction from the test result is no healing being observed in case of PCS samples, since no microbial species were introduced and also points out the fact that natural healing alone is insufficient for crack filling.

Secondly, mere introduction of bacterial species without an immobilizer yields partial healing and that water cannot act as an immobilizer for bacteria which will hamper long term survival of bacteria.

The test results also show that with increasing char content the healing efficiency has improved and maximum of 4 mm crack is healed in case of BIC 0.75. But at this point, we cannot say BIC 0.75 is optimum char concentration sample since the crack induction through UTM is not a controlled process. If BIC 1.00 was exposed to greater crack widths (> 4 mm) it may have healed that crack as well.

Another important supposition that can be made is a particular range of bacterial concentration results in effecting crack healing which can be verified through Energy Dispersive Spectroscopy (EDS). Bio-influenced self-healing can repair nonstructural and structural cracks, moreover past studies were confined to remediation of micro cracks (< 0.7mm) but bacterial immobilized char concrete has the capacity to repair macro cracks (> 0.7 mm).

4.1.2 Energy Dispersive Spectroscopy

EDS is employed to critically study the relation between carbonized waste char concentration and healing efficiency, a relationship that cannot be established through optical microscopy. This test involves elemental characterization of compounds present within the concrete matrix, most importantly calcium ions that is elemental component of calcite. For this test a chip was extracted from the healed surface from the specimen. It is worthy to note that chip obtained from any other surface would represent calcium ions due to hydration of cement only. So, we can safely say that the calcium ion concentration obtained from EDS results depicts its concentration in calcite only.

The following figures illustrate elemental compositions of the chips extracted from different concrete samples analyzed at multiple spectrums.

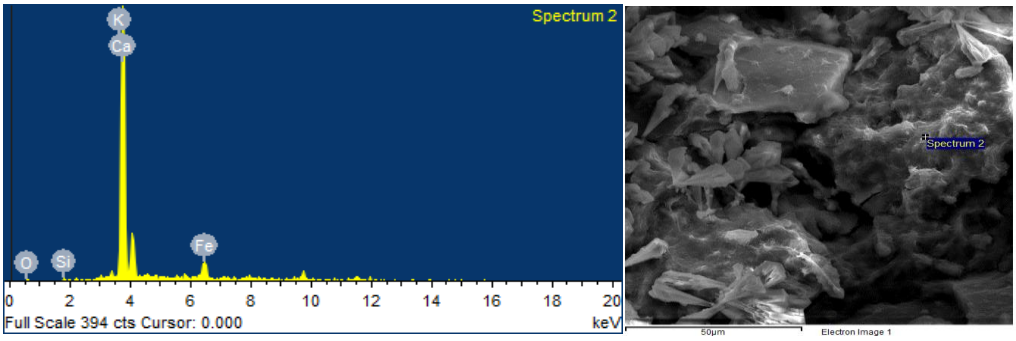

Figure 19: EDS of BCS at 50 µm

Table 11: Elemental composition of BCS

Element	Ca	Fe	O	K	Si	Mg	Al
Weight %	75.63	11.78	10.85	0.95	0.61	0.15	0.02

From the test result, we can conclude that BCS concrete has large reservoir of calcium ions that would then preserve its alkalinity.

4.1.3 Thermogravimetric Analysis

TGA is thermal analysis technique to identify different crystalline compounds in the cementitious matrix based on their decompositions at different temperatures. The change in mass in accordance with an increase in temperature, from 0 to 900°C gives the quantity of compound present. The TGA plot can be divided into 3 segments, first from 0 to 100°C corresponding to water. From 100 to 600 °C refers to ettringite that is a hydration product of concrete. Isfahani (2016) in his research findings identified temperature range from 400 to 500 °C for portlandite mass loss. Moreover, Warda Ashraf (2017) quoted 773.2 °C to be calcite burning temperature. We investigated temperature range 600 – 850 °C, the percentage change in the mass was observed referring it to amount of calcite present within the different concrete formulations.

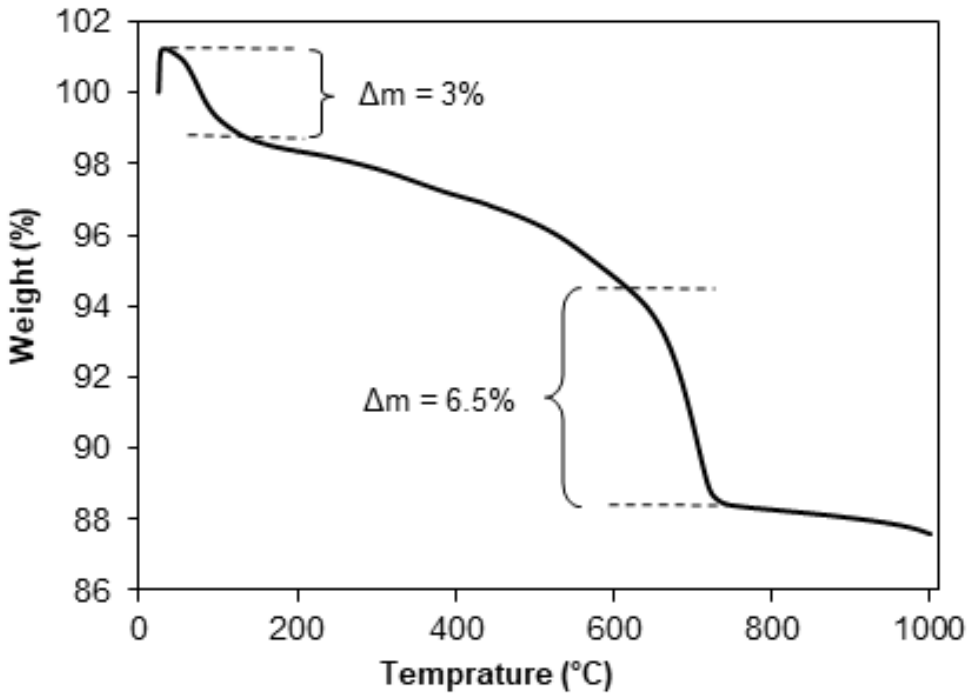

Figure 20: TGA of BCS 0.25

The change in mass (3%) in the temperature range 0-180 °C, represents the mass of unburnt cement. Whereas the change in the mass (6.5%) in the temperature region 600-850 °C, corresponds to calcite decomposition.

4.1.4 X-Ray Diffraction Analysis

XRD analysis involves phase identification of crystalline material to distinguish elemental components in self-healable concrete. For this test, a core was extracted from healed samples and relative peaks corresponding to specific elements is obtained.

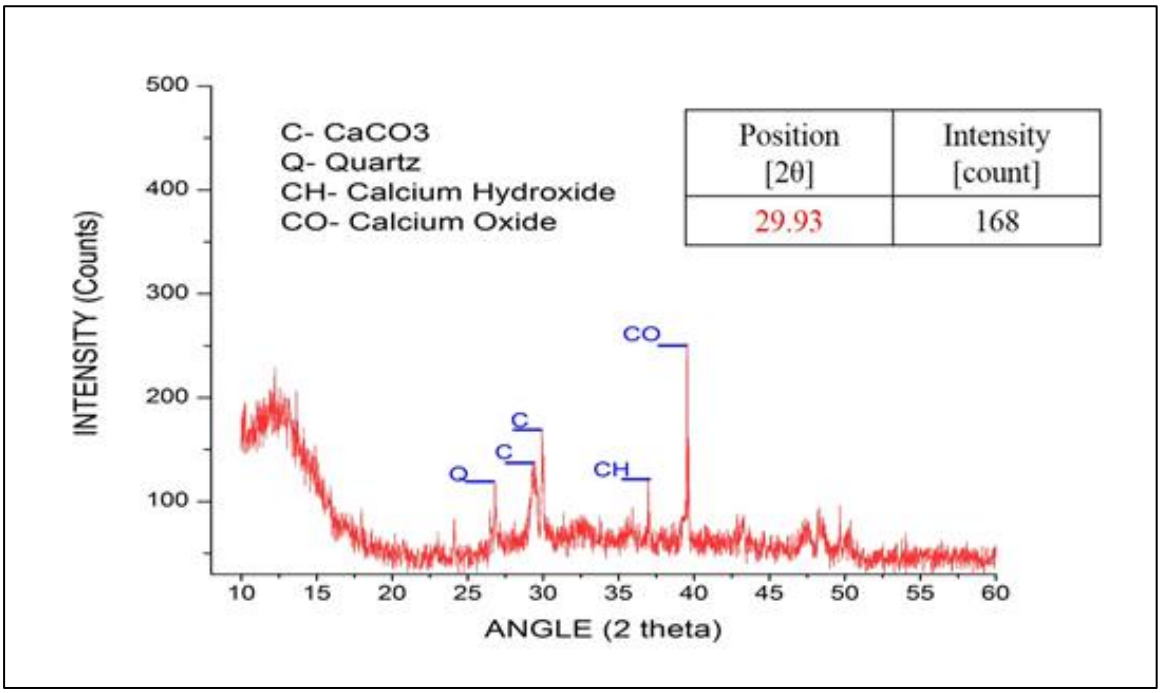

Figure 21: XRD of BCS 0.75

4.1.5 Strength Recovery Index

Bio influenced self-healing concrete not only fills the cracks but has the potential to restore the mechanical properties such as its compressive strength, lost after initiation of crack. Strength recovery index (SRI) represents strength regained after healing action in terms of percentage of its initial strength using the following formula.

$$SRI = \left(1 - \frac{Initial\ strength - Regained\ strength}{Initial\ strength}\right) x\ 100$$

The graphs below show the initial compressive strengths of the concrete at curing periods of 3, 14 and 28 days respectively. It is observed that with introduction of bacterial immobilized char the healing efficiency has improved that results in densification of concrete matrix enabling it to withstand increased loads until BIC 0.75. There is drop in compressive strength for BIC 1.00 because of agglomeration of char particles which leads to formation of weak zones that causes decrease in ability to sustain load hence lower compressive strength.

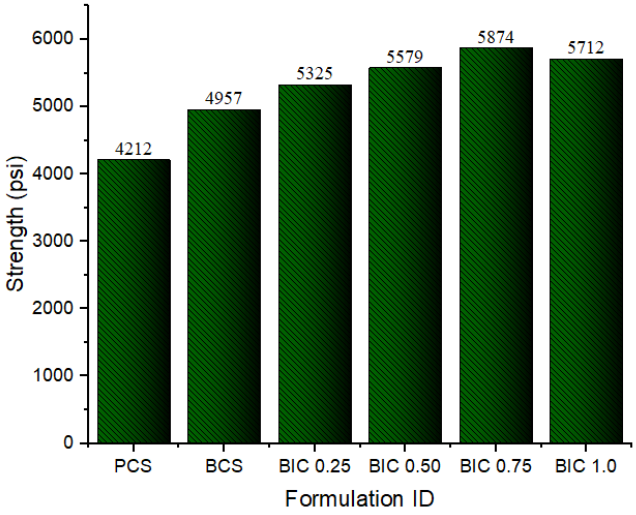

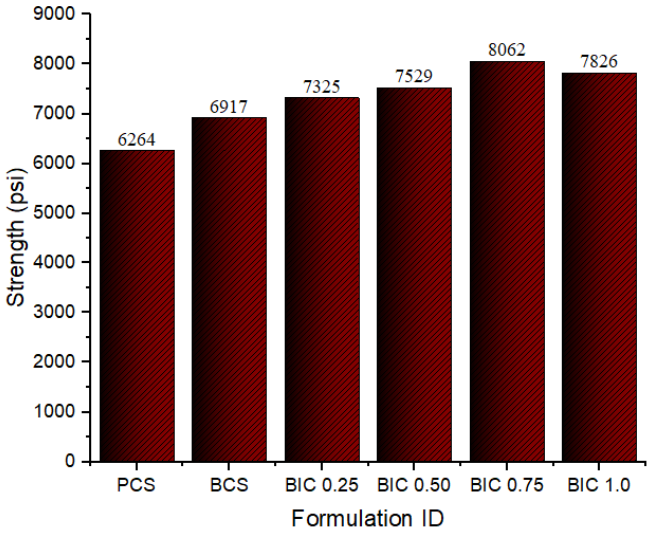

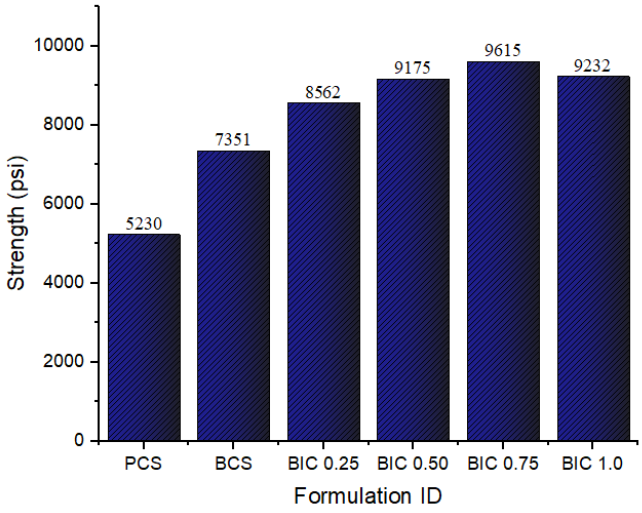

Figure 22: Compressive strengths at (a) 3 days (b) 14 days (c) 28 days, of cured samples

Generally, the strength recovered in the samples ranges from 40 to 90 % of its initial strength. The matrix figure below shows strength recovered against respective cured periods. The maximum of 96.3% strength recovery was observed.

3 Days	PCS	BCS	BIC 0.25	BIC 0.50	BIC 0.75	BIC 1.0
14 Days	PCS	BCS	BIC 0.25	BIC 0.50	BIC 0.75	BIC 1.0
28 Days	PCS	BCS	BIC 0.25	BIC 0.50	BIC 0.75	BIC 1.0

Below 40 %	41-50%	51-60%	61-70%	71-75%	76-80%	81-90%	Above 90%

Figure 23: Strength recovery matrix for different formulations

4.1.6 Ultrasonic Pulse Velocity

UPV test was carried to monitor the healing activity within the concrete samples cured at respective periods, for which the internal cracks were filled. In order to estimate the healing activity UPV was performed before cracked, then for pre-cracked and later for healed samples. Three methods were employed direct, semi-direct and indirect to investigate healing in different planes. Subsequent table depicts the velocities through concrete samples, in general the velocity increase with filling of cracks as there is no obstruction for waves to propagate.

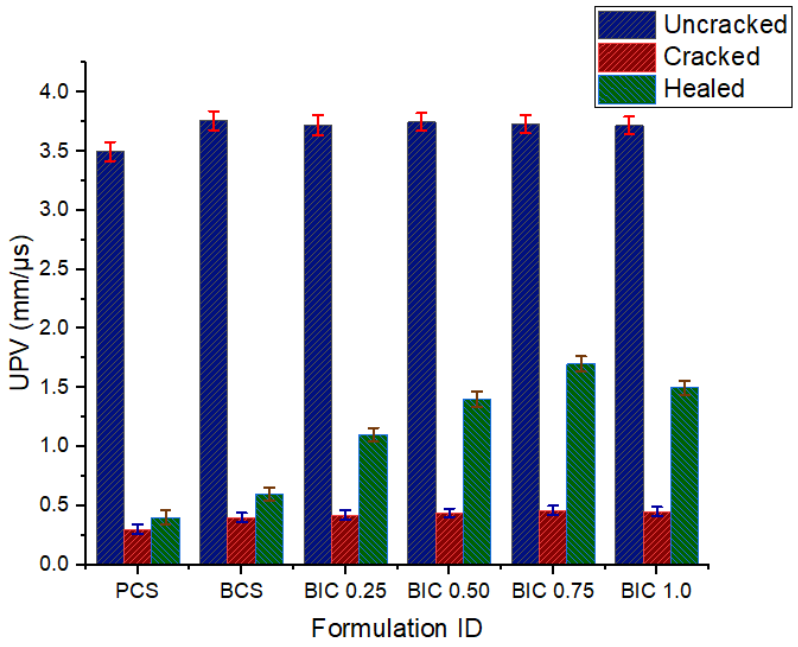
Uncracked
Cracked
Healed
UPV (mm/µs)
4.0
3.5
3.0
2.5
2.0
1.5
1.0
0.5
0.0
PCS
BCS
BIC 0.25
BIC 0.50
BIC 0.75
BIC 1.0
Formulation ID

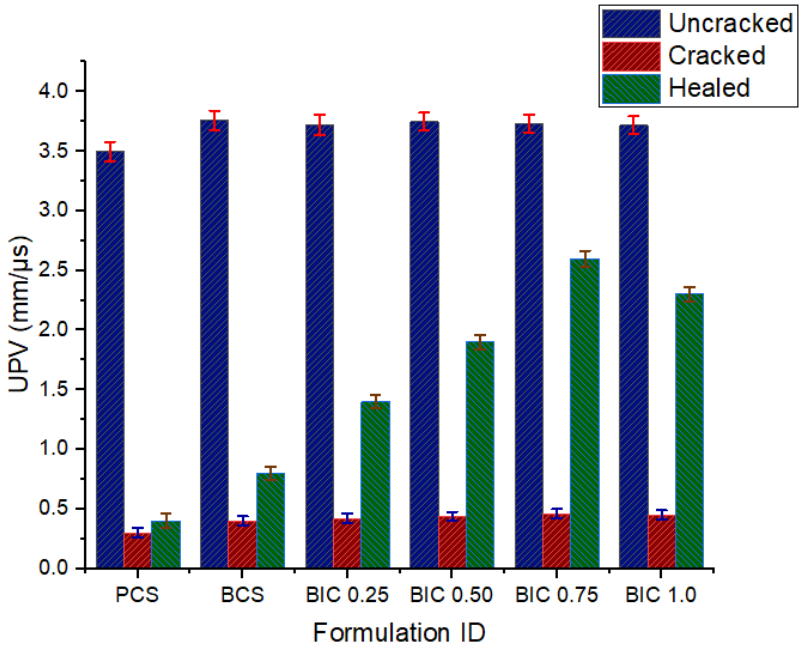
Uncracked
Cracked
Healed
UPV (mm/µs)
4.0
3.5
3.0
2.5
2.0
1.5
1.0
0.5
0.0
PCS
BCS
BIC 0.25
BIC 0.50
BIC 0.75
BIC 1.0
Formulation ID

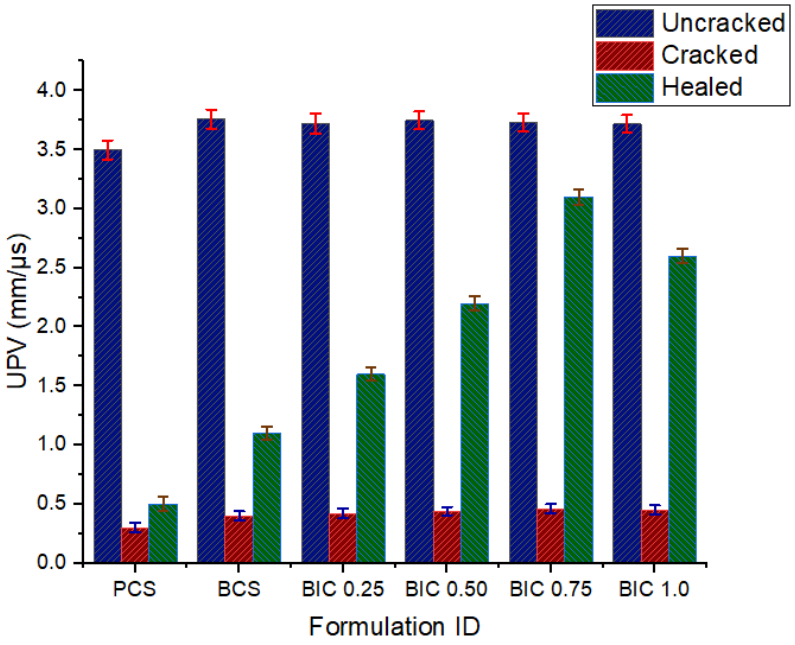

Figure 243: UPV on (a) 3 days (b) 14 days (c) 28 days, uncracked, cracked and healed samples

The results of UPV compliment the previous test results for healing. It can be seen that with increase char content the heeling efficiency has improved that results in crack repair therefore the speeds have increased through the transducers.

4.2 CORROSION

4.2.1 Non-Steady State Chloride Ion Migration

The test was executed under NT-BUILT 492, for which un-reinforced concrete cylinders were cut into 2 in discs using diamond saw, after which the discs were stored in the for preconditioning in the vacuum chamber by exposing both end surfaces for vacuum treatment. Later the pressure was dropped to 3 kPa in a matter of few minutes inside the chamber and then kept constant for 3 hours. Then fill the container with saturated $Ca(OH)_2$ solution with all samples fully immersed for a period of one hour before entry of air was allowed into the container for a further 18 hours.

Since the test is based on an electrochemical cell it requires an anode and a cathode. The catholyte solution was 10 % NaCl by mass in water whereas the anolyte solution was 0.3 N NaOH in distilled water, kept at 25 °C during the test.

Catholyte reservoir was filled with 12 L of catholyte solution and the concrete discs were wrapped around a rubber sleeve tightly. The concrete disc was fixed on the plastic support fitted in the catholyte reservoir, remaining sleeve filled above the disc with 300 ml anolyte solution and anode was dipped in it. Cathode with the negative terminal and anode with the positive terminal was connected with the power supply.

For the migration test, power supply was switched on with the voltage assigned 30 V and note the initial current and temperature through each formulation. As per the standard specifications, the test duration was set 20 hours after which the test is completed by recording the final current reading and temperature.

Second phase of this test involves the computation of the depth of chloride penetration for which the concrete discs were split into half axially and sprayed 0.1 M silver nitrate solution. When white precipitate of silver chloride was observed, the depth of penetration was recorded using scale from center to edges at reasonable interval and later mean was determined.

Figure 25: Sample preparation using diamond saw cutter

Figure 264: Sample isolation through vacuum chamber

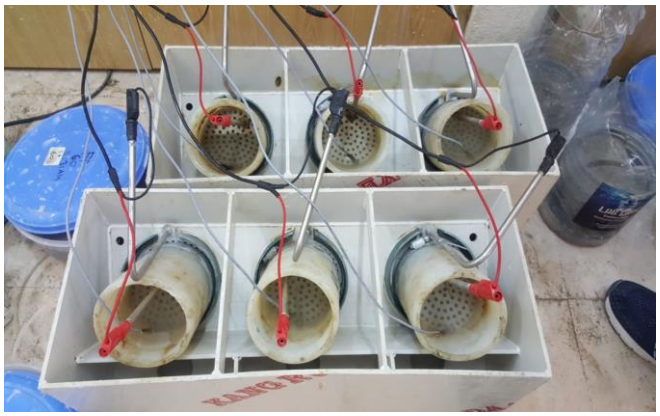

Figure 27: Potential applied via catholyte reservoir

Figure 285: Voltage drop monitoring through potentiostat

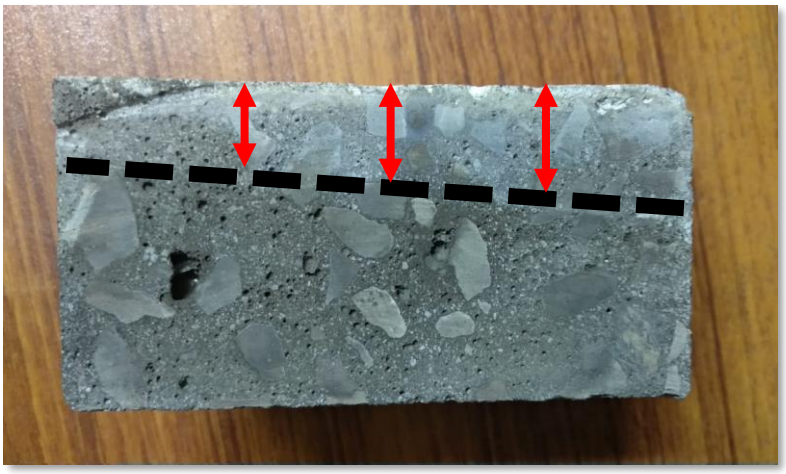

Figure 29: Measurement of chloride penetration depth

The non-steady state migration coefficient was calculated using the following equation

$$D_{ssm} = \frac{0.0239(273+T)L}{(U-2)t}\left(x_d - 0.0238\sqrt{\frac{(273+T)Lx_d}{U-2}}\right)$$

Where,

D_{ssm} : non steady state migration coefficient, x 10^{-12} m^2/s;

U: applied voltage, V;

T: mean of initial and final temperatures in the anolyte solution, °C;

L: thickness of concrete discs in mm;

x_d: mean of penetration depths at different intervals, mm;

t: test period, hour.

The graph below represents the migration coefficient values for various formulations. It can be implied that bacterial inspired concrete reduces the attack of aggressive agents like chloride ions by filling the pores whilst making the concrete impermeable. With increase in char content the healing activity increases that decreases the corrosion within the samples by 89%.

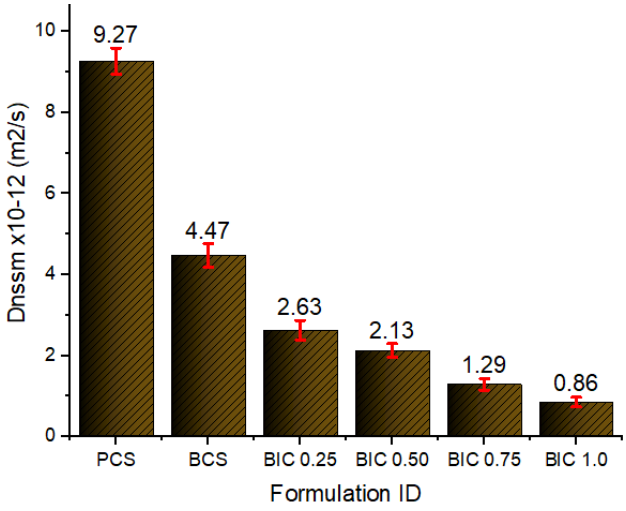

Figure 30: Migration coefficients for different formulations

4.2.2 Sorptivity Test

To conduct this test according to ASTM C1585, the concrete discs having 2 in depth were pre-conditioned using vacuum desiccator placed inside an oven at 50 °C for 3 days. Initial mass recorded, after which specimens were placed inside a sealable container for 15 days at room temperature, with precautionary measures taken to allow free flow of air without touching the sides of container.

Specimens were withdrawn from the container and pre-conditioned after sealing the sides with plastic sheet. The schematics shown in the figure below was employed to measure the absorption for which a support system was provided and the tap water was filled up to 1 mm above the support system. Then the test surface of the concrete discs was placed on the support system and stopwatch being started. The time intervals were kept as per the standard are summarized in the table below and prior to weight measurements, the specimens were cleaned using towel with timer on stopwatch being stopped.

Table 12: Time intervals as per ASTM C1585

Time	60 s	5 min	10 min	20 min	30 min	60 min	Every hour up to 6 h	Once a day up to 3 days	Day 4 to 7 three readings 24 h apart	Day 7 to 9 one reading
Tolerance	2 s	10 s	2 min	2 min	2 min	2 min	5 min	2 h	2 h	2 h

To calculate absorption following formula was utilized

$$I = \frac{m_t}{a * d}$$

Where,

Figure 31: Concrete samples immersed in NaCl solution

I: the absorption;

m_t: change in mass of concrete discs, at time t;

a: the surface area of specimen in contact with water, mm^2;

d: density of water, g/mm^3.

Initial rate of absorption ($mm/\sqrt{s}$) was determined by drawing the line of best fit through linear regression equation for the plotted points as shown in the graph below.

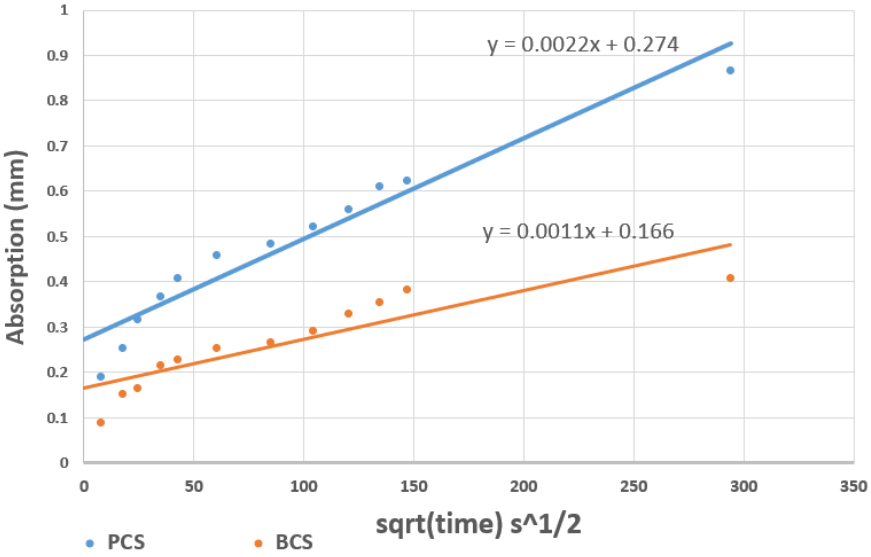

Figure 32: Plot of best fit line for sorptivity

The bar chart shown in the figure below summarizes the absorption rates for different formulation, it can be observed that healing action reduces the permeability in the concrete hence the carbonation within concrete is prevented that ensures the reinforcement is preserved. The calculation reveals 68 % decrease in permeability for BIC 0.75 relative to PCS.

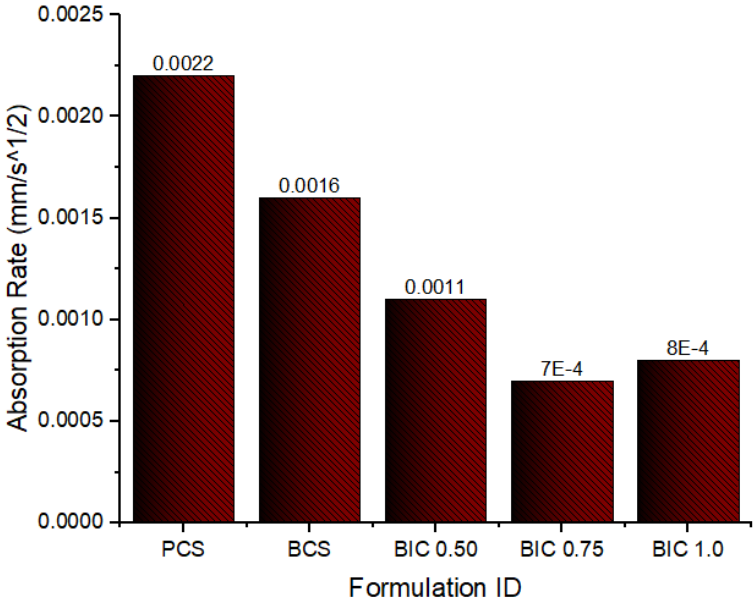

Figure 33: Absorption rate for different formulations

4.2.3 Tafel Polarization

Tafel Polarization test was performed under ASTM G-59 to determine the corrosion rate of the embedded reinforcement in the cylindrical concrete samples. It is a faster experimental technique as compared with the classical weight loss measurement.

The concrete samples cured for 28 days were immersed in 3.5% NaCl solution for a period of 12 days. Gamry Potentiostat determines the corrosion rate of the reinforcing steel. Apparatus consist of three electrodes as shown in the figure:

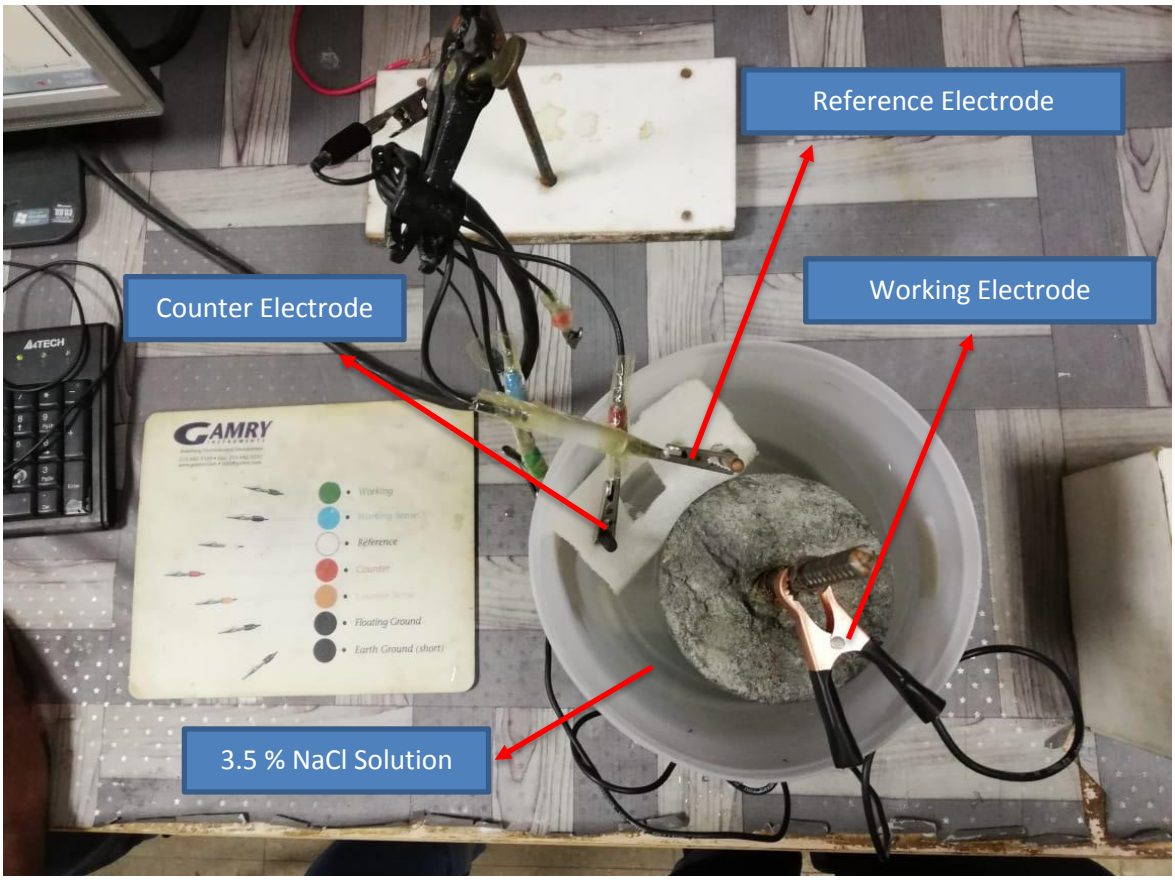

Figure 34: Schematics of tafel polarization

i). Working Electrode: Reinforcing steel acts as working electrode (corrosion rate of which is to be determined).

ii). Reference electrode used was copper (E_{corr} was measured with respect to copper's potential)

iii) Counter electrode used was of graphite to complete the electrochemical cell due to its inert property.

After the whole assembly was set up, the potential scan of ± 250 mV about E_{corr} so that reasonably accurate extrapolation can be made to the corrosion potential. The curve was plotted between current on x-axis vs potential on y-axis. Cathodic and anodic reactions occur simultaneously on the surface of rebar. At first, the working electrode acts as cathode and the cathodic region of the curve depicts this behavior. When the electrode reaches its corrosion potential, the working electrode then starts to act as an anode and the anodic curve is obtained. The corrosion rate of the reinforcing steel was acquired by Tafel extrapolation method as shown in the graph.

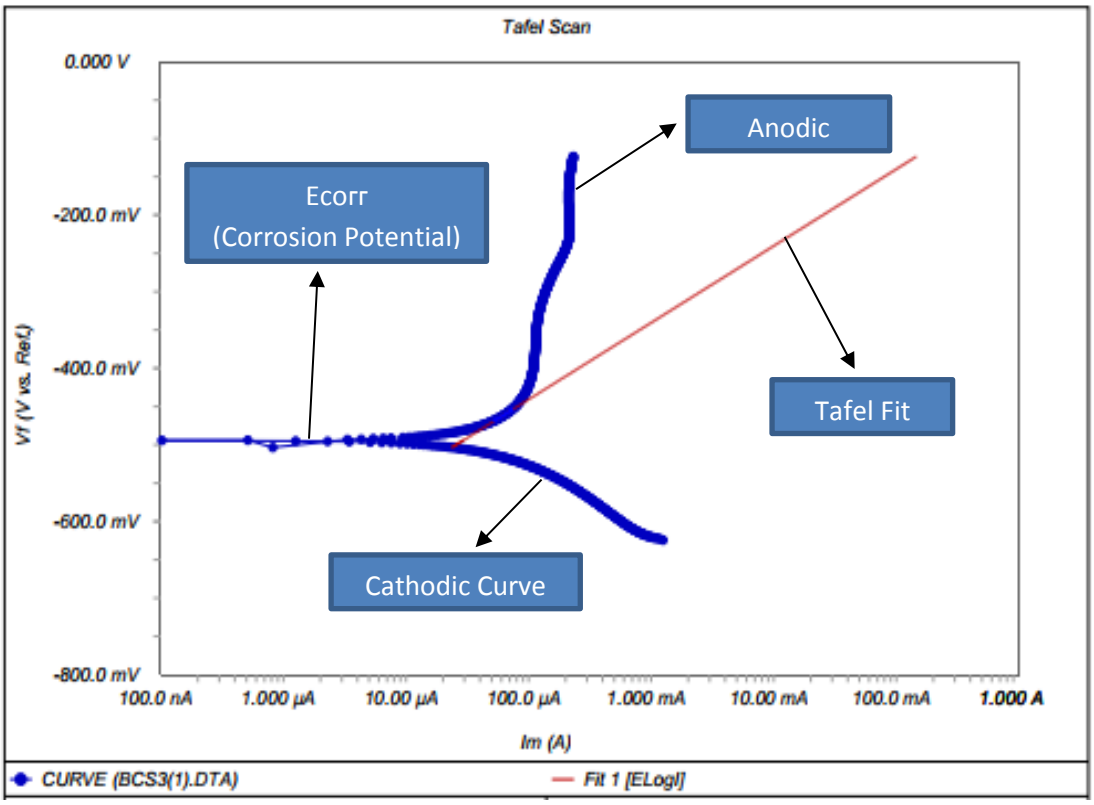

Figure 35: Tafel plot obtained from GAMRY software

The general trend of different concrete formulations is shown in the graph followed by figure summarizing the test result.

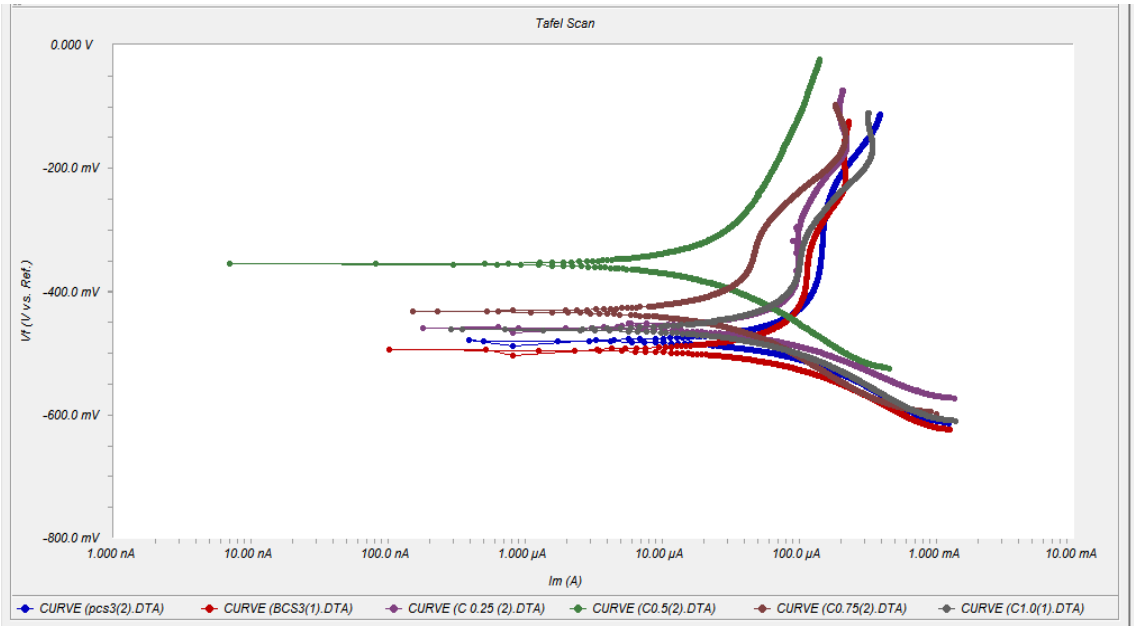

Figure 36: Superimposed curves of tafel plot

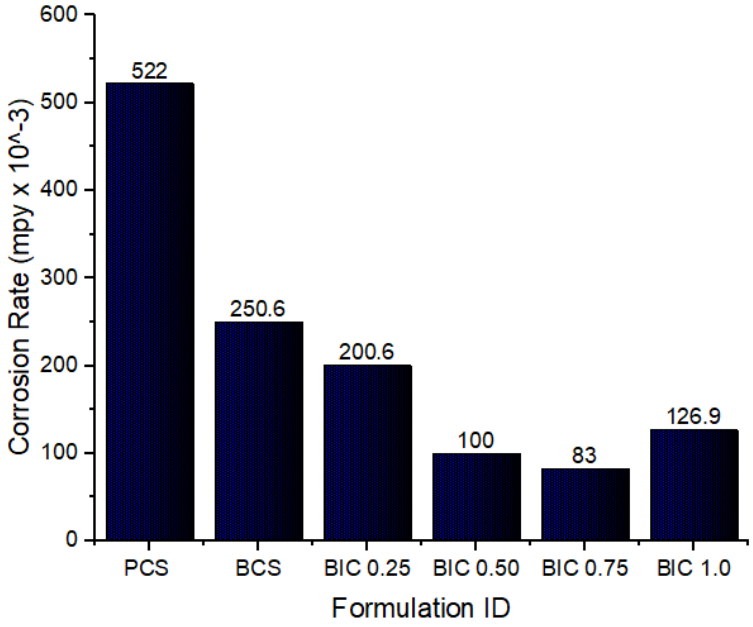

Figure 37: Corrosion rate through tafel fit

As the healing activity is maximum in case of BIC 0.75, therefore the corrosion is minimum, about 84 % lesser as compared to PCS, as can be seen from the above test result and complimented by previous test results. The corrosion, as expected, is maximum in PCS sample, as the porosity is high for chloride ions to penetrate for the corrosion process to initiate. With introduction of microbial species, the porosity is reduced by filling the micro-cracks through calcite precipitation hence preventing potential corrosion. Slight increase in corrosion rate at biochar of 1 % is due to the

non-effective dispersion of biochar in the concrete that leads to the clumps formation, resulting in inefficient healing hence increased corrosion rate.

4.2.4 Weight Loss Measurement

Weight loss measurement is a classical technique to determine the corrosion rate of the rebar in the concrete samples. Weight of the rebars before casting was noted using balance with accuracy of up to 0.1 g. The same cylindrical samples with rebar at its center were casted and were placed for curing. After the 28 days curing period, the samples were dipped in 3.5% NaCl solution and a DC supply of 12 V was applied for 12 hours. The Samples were then broken down and the corroded bars were cleaned using both mechanical and chemical methods.

In mechanical method, the sponge was used to remove the corrosion products. In chemical method, the bars were immersed in 20 % w/w solution of NaOH with 2 % granulated zinc for 40 minutes at 85°C according to the standard ASTM G1-03.

Figure 38: Pictorial description of weight loss measurement test

The weights of bars after washing was measured and change is mass of the bars were calculated to find the percentage of corrosion for different formulations as shown in the following graph.

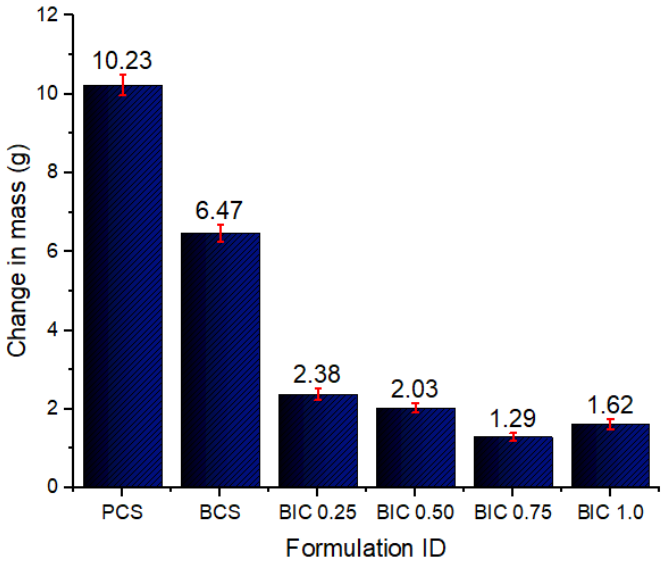

Figure 39: Weight loss measurement results

The change in mass corresponds to the amount of corrosion in the concrete specimens with maximum corrosion observed in case of PCS and least evident in BIC 0.75 (almost 90 % less as compared with PCS). The test result is identical to previous tests which supports the hypothesis of self-healing concrete repairing micro-cracks rendering the concrete impermeable to chloride and carbonation agents which triggers corrosion in the embedded concrete reinforcement.

4.3 CO_2 Monitoring

Bio-influence self-healing concrete essentially absorbs CO_2 in the calcite precipitation. Studies conducted in the past were centered around the crack healing potential and effects on mechanical properties with no efforts made to quantify the CO_2 sequestration ability of the self-healable concrete. In addition, the bio-char used to immobilize bacteria has the ability to adsorb CO_2.

4.3.1 Climate Controlled Chamber

Therefore, to measure the amount of CO_2 absorbed by different formulations of concrete in this research, a customized climate control chamber was assembled with its schematics displayed in the following figure.

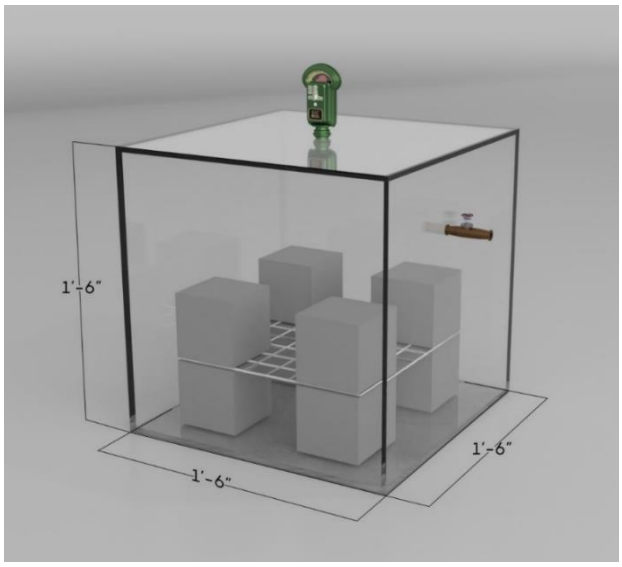

Figure 40: Schematics of climate control chamber

Figure 41: Real time CO_2 monitoring in the climate control chamber

As seen, chamber is a cuboid having a length of 1.5 feet made of 6 mm acrylic glass. Mounted on the top is EXTECH sensor that records CO_2, temperature and humidity with time. The sensor can be time calibrated with minimum stage of 1 minute with its probe suspended inside the chamber. The sensor comes along with a data logger that continuously records the readings, as per the stage set, in an excel file which can be retrieved through the memory card fitted inside the sensor.

On one of the sides of the chamber, a 0.25 in dia valve was installed to allow the entry of CO_2. CO_2 gas was inserted via ignition of match stick because the direct entrance through CO_2 cylinder would damage the sensor with fears of chamber being blown up under high pressure of compressed CO_2 gas in the cylinders.

To ensure that the entrapped CO_2 does not leak into atmosphere the sides of the chamber was lined through silicon sealant internally and externally the edges were covered with scotch tape. Eight concrete samples were placed in the chamber of four different formulations with a steel mesh placed between samples to adjust the space covered inside the chamber by concrete.

The underline methodology was to raise the concentration of CO_2 within the chamber up to maximum of 4000 ppm and monitor changes in concentration to reach a minimum threshold of 100 ppm. The graph below shows the concentration of CO_2 against time. The char-controlled sample (CCS) bears only 1.5% bio char which is not immobilized with bacteria with a view to investigate the CO_2 adsorbing potential of CWT char.

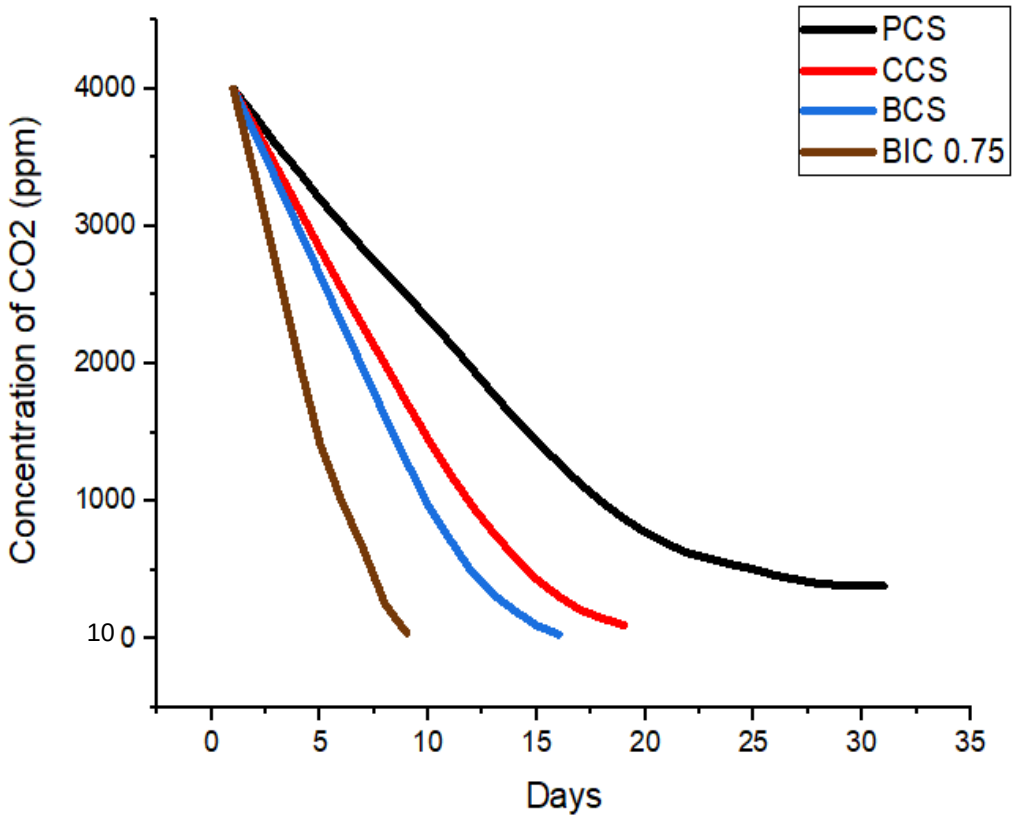

Figure 27 : CO_2 monitoring result extracted from sensor

The PCS sample took 29 days to reach a saturation point of 300 ppm which implies that it has reached its maximum ability to absorb CO_2. Moreover, this intake of CO_2 is detrimental to concrete as it causes carbonation which leads to corrosion as evident from phenolphthalein test result shown in the figure below. The purple area represents section unaffected by carbonation whereas grey area shows carbonation depth.

Figure 43: Phenolphthalein Test for PCS

The BCS concrete reached the minimum threshold in period of 16 days due to fact that microstructural crack filling takes place as result of bacterial action consumes CO_2.

The CCS sample has the tendency to adsorb CO_2 as endorsed by literature (Gupta, 2017) but compared to BCS sample its uptake potential is less.

With the introduction of bio immobilized char, the CO_2 sequestration ability of concrete has increased drastically as can be inferred from the above graph that the BIC 0.75 has the highest potential to inhale CO_2 taking only 8 days to reach minimum threshold of 100 ppm. The phenolphthalein test shown in the figure below testifies that this absorption of CO_2 will not cause corrosion in the reinforcement embedded within concrete.

Figure 448: Phenolphthalein test for BIC 0.75

4.3.2 Room Model

In order to study the environmental impact of bio influenced self-healing concrete reasonably it is imperative to model the concrete on a grand scale for which a hypothetical room was designed as displayed in the figures below.

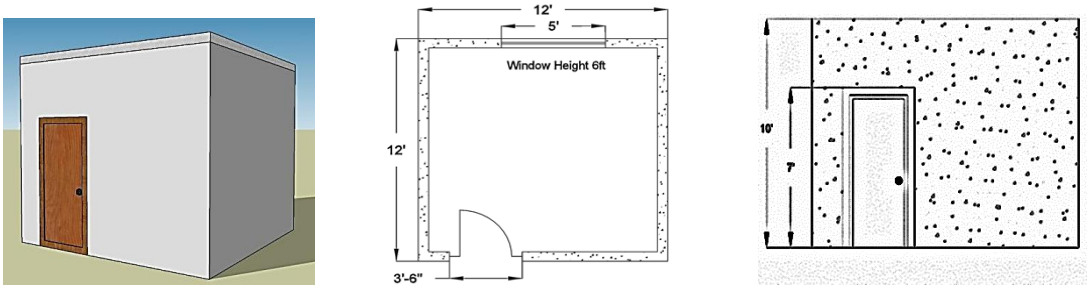

Figure 45: Hypothetical room model (a) elevation (b) plan (c) front view

The square room has dimension of 12 feet with a door and window placed on the opposing faces. In order to calculate the absorbing capacity of the room, it is assumed that walls and slab is made of BCS concrete, the interaction of soil is neglected hence foundations are not accounted for in the calculation. Similarly, additional factors such as population density, green lands, social-economic activities like setting up of industry and urbanization are not considered, therefore the calculations only represent ideal conditions which have been summarized in the table below.

Table 13: Summary of room model calculations

Volume of room	11100203 cm^3
CO_2 absorbed by the model	217009 cm^3
CO_2 absorbed/ cm^3 of concrete	0.0195 cm^3

CHAPTER 5

FIELD TRIAL

5.1 Introduction

Through past researches it has been established that bio-influenced self-healable concrete works efficiently in live concrete but the performance of bio-based products such as bio-emulsion in dead concrete is yet to explored and has become research interest for many researchers most recently. Conventional crack filling techniques such as epoxy grout are prevalent in construction sector, but pose potential problems such as durability, as cracks appear to propagate from very same location after couple of years, moreover it is costly crack repair method requiring specialized staff.

Bio-emulsion comprises of typical grout ingredients (cement, sand and water) and in addition bacterial solution and bio-char. Cement sand ratio was kept 1:1.9, whereas 0.45 water cement ratio was selected to achieve consistency through trial and error. The percentages of bacterial solution and bio char was designated 3% and 0.75% respectively.

Epoxy grout used in this research study was commercial epoxy. The chemical-water ratio was kept 3:1 as per the manual provided by the company with resin injected at the mid-point of the grid.

5.2 Procedure

In order to draw comparison between bio-emulsion and epoxy grout, NIT (NUST) car parking, was selected as test site possessing macro cracks in its pavement as shown is the figure below.

Figure 46: Site selection NIT (NUST) car parking

After which a 1 feet square grid was plotted, figure x.w.1, with the crack lying in the center of the grid. Then the crack was cleaned using a broom to remove dust, and to have an idea of exact width and depth of the crack.

UPV values across the grid were noted as seen in the figure below and later one crack was filled with bio-emulsion and epoxy grout was applied over the other.

The crack was cured using jute bags for period of 7 days, afterwards UPV readings were taken at respective grid points.

Figure 47: Pictorial description of field trial

5.3 Results

The figures below summarize the results of UPV readings converted into speeds.

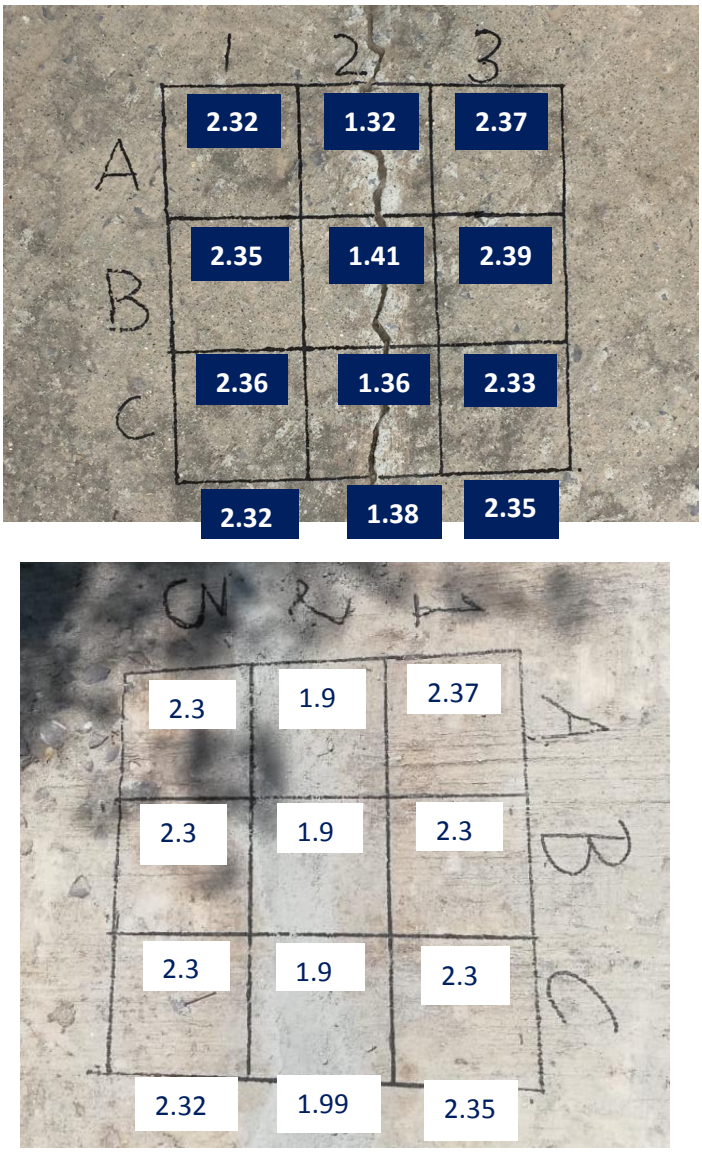

Figure 48: UPV results (a) before (b) after application of epoxy grout

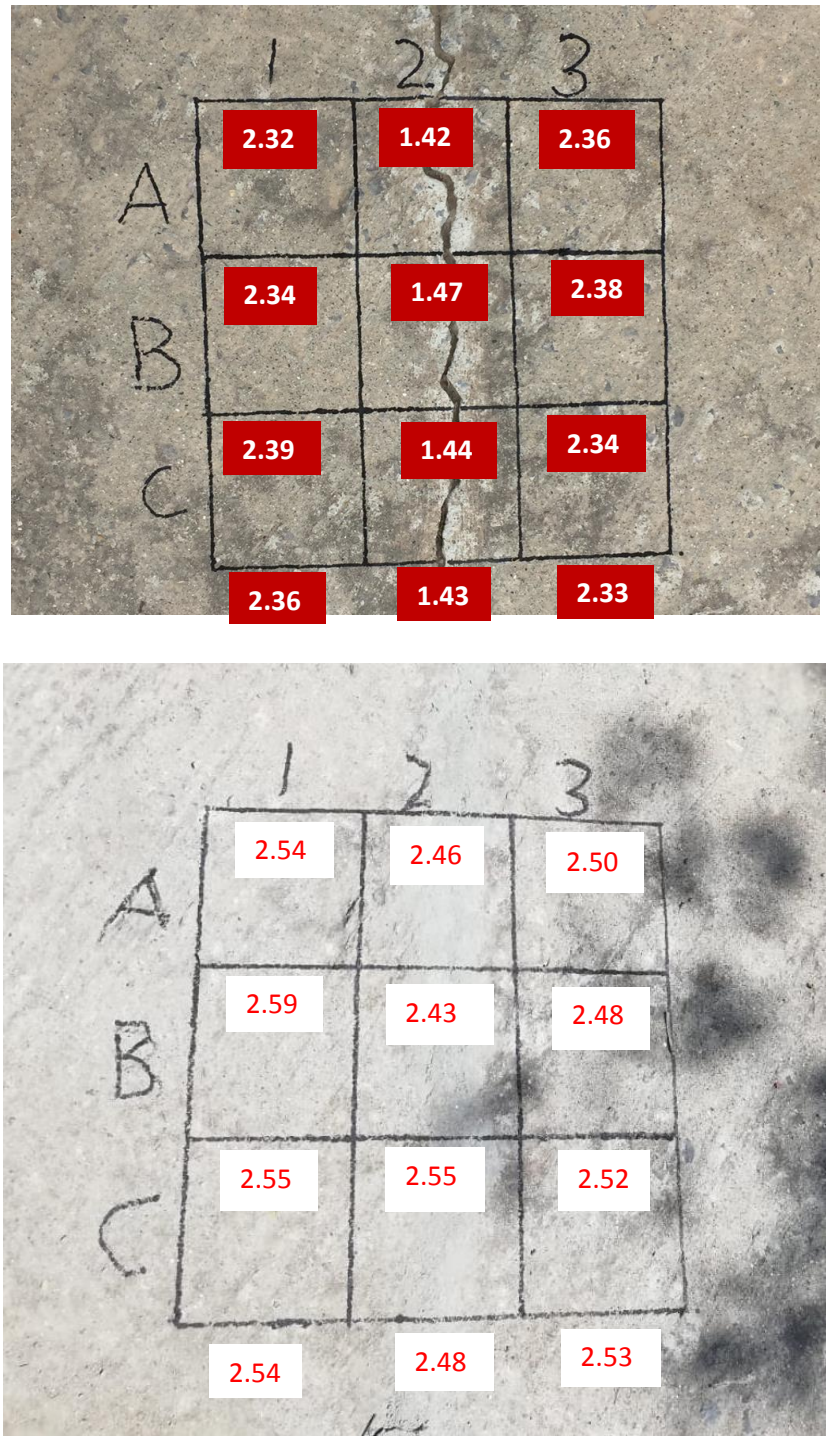

Figure 49: UPV results (a) before (b) after application of bio-emulsion

The underline theory of UPV, as discussed in healing portion, any cracks present within the structure reduces the speed as they provide barrier to the flow of ultrasonic waves. The differences in the speed before and after the application of epoxy grout shows that crack has filled significantly.

But in comparison with bio-emulsion, the difference in speed is lesser for epoxy grout that proves bio-emulsion is better crack filler. Moreover, the adjacent concrete matrix has also improved in the case of bio-emulsion with the reason being intrusion of bacterial species in surrounding concrete unit and improving it by filling microstructural cracks leading to densification of concrete matrix.

5.4 Cost Comparison

Quantities to prepare 1 kg mix were worked out and accordingly the price incurred calculated as shown in tables below from which it can be deduced that bio-emulsion is 10 times cost effective solution as compared to epoxy grout.

Table 14: Cost estimation of bio-emulsion

Material Quantities			Market Rate	Price (PKR)
Item	Quantity	Unit		
Cement	0.345	Kg	600/bag	281.0
Sand	0.655	Kg	20/cft	75.2
Calcium Lactate	0.010	Kg	3700/kg	38.3
Bacteria	0.014	Kg	-	-
Nutrient Broth	0.0153	Kg	6000/L	92
			Total	486.5

Table 1514: Cost estimation of epoxy grout

Ratio	**3:1**
Quantity	0.75 kg
Market Rate	7000/kg
Total	5250 Rs.

CHAPTER 6

CONCLUSIONS

1. Biochar serves as an effective immobilizer for long term survival of bacillus subtilis specie having maximum healed crack width of 4.0 mm with highest strength recovery of 96.3% at 28 days curing period
2. CO_2 sequestration ability of CWT immobilized with bacteria is 3 times the normal concrete
3. Bio-inspired Self-Healing concrete reduces the diffusion coefficient almost 10 times and rate of corrosion up to 82% thus enhancing the immunity to corrosion
4. Replacing cement by 0.0075 times with CWT, optimum healing and resistance to corrosion is observed
5. Prepared bio-emulsion proves to be an effective and cheap repairing technique in dead concrete regarding the micro-structural improvement of adhering concrete

RECOMMENDATIONS

1. Analyze the effect of varying curing periods on the rate of corrosion
2. Study the effect of voltage applied in case of corrosion tests on the bacterial species survival
3. Monitor the effects of temperature increase on the healing efficiency
4. Investigate the fracture mechanics of self-healing concrete immobilized with carbonized waste tire to study its structural response
5. Numerical modelling of the mentioned concrete through software like Etabs must be carried out to analyze linear and nonlinear behaviour of structure under applied loads
6. Mechanism or modelling using equipment/software must be developed for real time monitoring of corrosion to prevent further deterioration of structure
7. Effects of humidity must be studied in detail on CO_2 sequestration ability of concrete as humidity and CO_2 concentration are inversely related with each other
8. Environmental impact must be studied in detail on large scale by incorporating factors such as urban sprawl, growing population and socio-economic activity
9. Study was conducted on uncracked specimen; the horizon of research should be extended to cracked concrete samples so as to draw meaningful comparison between the CO_2 sequestration potential of concrete
10. Further investigation is required to evaluate the performance of bio-emulsion in dead concrete for which forensic testing is required
11. Prolong periods of examination of UPV values must be done to validate long term durability of bio-emulsion

CONSTRAINTS

1. Difficulty in extracting images from crack width measurement as the instrument is outdated
2. Capacity constraints of temperature-controlled curing tank limits number of samples to be casted for testing
3. Lack of molds prevent large scale casting; hence the casting regime must be extended so does the testing with difficulty in maintaining testing record
4. Field trail procedure must be improved as time limitation could only focus on short term analysis with forensic evaluation pending

REFERENCES

Wasim Khaliq, Muhammad Basit Ehsan, Crack healing in concrete using various bio influenced self-healing techniques, Construction and Building Materials 102 (2016)

Sini Bhaskar 2016, Self-Healing Bacterial Cementitious Concrete Composites: Development and Performance Evaluation

H.M. Jonkers, A. Thijssen, G. Muyzer, O. Copuroglu, E. Schlangen, Application of bacteria as self-healing agent for the development of sustainable concrete, Ecol. Eng.36 (2) (2010)

J. Y. Wang, N. De Belie, W. Verstraete, 2012, Diatomaceous earth as a protective vehicle for bacteria applied for self-healing concrete

Van der Zwaag, S., van Dijk, N.H., Jonkers, H.M., Mookhoek, S.D., and Sloof, W.G., (2009), Self-healing behaviour in man-made engineering materials: bio inspired but taking into account their intrinsic character"

Ghosh, P., Mandal, S., Chattopadhyay, B.D., and Pal, S., (2005), "Use of microorganism to improve the strength of cement mortar"

Self-Healing Materials, 2010, Martin D. Hager , Peter Greil , Christoph Leyens , Sybrand van der Zwaag , Ulrich S. Schubert

Van Tittelboom, K., De Belie, N., De Muynck, W., and Verstraete, W., (2010), "Use of bacteria to repair cracks in concrete"

Li, V.C., and Yang, E.H., (2007), "Self-healing materials: an alternative approach to 20 centuries of material science

Hirozo Mihashi1 and Tomoya Nishiwaki, 2012, Development of engineered self-healing and self-repairing concrete, Journal of Advanced Concrete Technology

Wang, J.Y., Van Tittelboom, K., De Belie N, and Verstratete, W., (2012b), "Use of silica gel or polyurethane immobilized bacteria for self-healing concrete"

S.K. Ramachandran, V. Ramakrishnan, S.S. Bang, Remediation of concrete using microorganisms, ACI Mater. J. 98 (1) (2001)

Hammes, F. And Verstraete, W., (2002), "Key roles of pH and calcium metabolism in microbial carbonate precipitation"

De Muynck, W., Cox, K., Belie, N.D., and Verstraete, W., (2008a), "Bacterial carbonate precipitation as an alternative surface treatment for concrete"

Bang, S.S., Galinat, J.K., and Ramakrishnan, V., (2001), "Calcite precipitation induced by polyurethane immobilised Sporosarcina pasteurii"

Sierra-Beltran, M.G., Jonkers, H.M., and Schlangen, E., (2014), "Characterization of sustainable bio-based mortar for concrete repair"

Palin, D., Wiktor, V., and Jonkers, H.M., (2014), "Towards cost efficient bacteria based self-healing marine concrete"

Achal, V., Mukherjee, A., Basu, P.C. and Reddy, M.S., (2009), "Lactose mother liquor as an alternative nutrient source for microbial concrete production by Sporosarcina pasteurii

Achal, V., Mukherjee, A. And Reddy, M.S., (2011), "Microbial concrete: A way to enhance the durability of concrete buildings"

Guadalupe Sierra-Beltran, M., Jonkers, H.M., and Schlangen, E., (2014), "Characterization of sustainable bio-based mortar for concrete repair"

Warda Ashraf (2016), Effects of High Temperature on Carbonated Calcium Silicate Cement (CSC) and Ordinary Portland Cement (OPC) Paste

Forood Torabian Isfahani (2016), Effects of Nanosilica on Compressive Strength and Durability Properties of Concrete with Different Water to Binder Ratio

Broomfield JP (1997). Corrosion of steel in concrete: understanding, investigation and repair.

Bentur A, Diamond S, Berke NS (1997). Steel corrosion in concrete: fundamentals and civil engineering practice

Dif Fodil, Mouli Mohamed (2018). Compressive strength and corrosion evaluation of concretes containing pozzolana and perlite immersed in aggressive environments

Tanvir Manzur, Bayezid Baten, Md. Jihan Hasan, Halima Akter, Adhora Tahsin, Khandaker M.A. Hossain (2018). Corrosion behavior of concrete mixes with masonry chips as coarse aggregate

Y. Zhou, B. Gencturk, K. Willam, A. Attar (2015). Carbonation-induced and chloride induced corrosion in reinforced concrete structures

M. Moreno, W. Morris, M.G. Alverez, G.S. Duffo (2004). Corrosion of reinforcing steelin simulated concrete pore solutions - Effect of carbonation and chloride content

Bertolini L, Elsener B, Pedeferri P, Polder R (2003). Corrosion of steel in concrete: prevention, diagnosis and repair

Hartt WL, Lee SK, Costa E (1998). Condition assessment and deterioration rate for chloride contaminated reinforced concrete structures

Amir Poursaee (2016), Corrosion of steel in concrete structures

Lim, J. L. G., Raman, S. N., Lai, F.-C., Zain, M. F. M., Hamid, R., Synthesis of nano cementitious additives from agricultural wastes for the production of sustainable concrete

Lim, J. L. G., Raman, S. N., Lai, F.-C., Zain, M. F. M., Hamid, R. (2018), Synthesis of nano cementitious additives from agricultural wastes for the production of sustainable concrete

Ahmad, S. (2018), Innovative mix design of cementitious materials for enhancing strength and ductility

Restuccia, L., Ferro, G. A. (2016), Promising low cost carbon-based materials to improve strength and toughness in cement composites

Adhikari, B., De, D., Maiti, S. (2000), Reclamation and recycling of waste rubber, Progress in polymer science

Farooq, M. Z., Zeeshan, M., Iqbal, S., Ahmed, N., Shah, S. A. Y. (2018), Influence of waste tire addition on wheat straw pyrolysis yield and oil quality

Martínez, J. D., Veses, A., Mastral, A. M., Murillo, R., Navarro, M. V., Puy, N., Artigues, A., Bartrolí, J., García, T. (2014), Co-pyrolysis of biomass with waste tyres: upgrading of liquid bio-fuel

Gaëtan Rimmelé, Véronique Barlet-Gouédard (2010) Accelerated degradation method for cement under CO2-rich environment:The LIFTCO2 procedure (leaching induced by forced transport in CO2 fluids)

H.S. Wong, A.M. Pappas, R.W. Zimmerman, N.R. Buenfeld (2011), Effect of entrained air voids on the microstructure and mass transport properties of concrete

Sormeh Kashef-Haghighi, Yixin Shao, Subhasis Ghoshal (2014), Mathematical modeling of CO_2 uptake by concrete during accelerated carbonation curing

Yves F. Houst I and Folker H. Wittmann (1994), Influence of porosity and water content on the diffusivity of CO_2 and O_2 through hydrated cement paste